N.M. Gerrits, T.J.H. Ruigrok and C.I. De Zeeuw (Eds.)
Progress in Brain Research, Vol 124

CHAPTER 11

Topography of cerebellar nuclear projections to the brain stem in the rat

T.M. Teune, J. van der Burg, J. van der Moer, J. Voogd and T.J.H. Ruigrok*

Department of Anatomy, Erasmus University Rotterdam, P.O. Box 1738, 3000 DR Rotterdam, The Netherlands

Introduction

The cerebellum has been implicated to be involved in motor control (Bloedel, 1992; Ito, 1984), cognition (Leiner et al., 1986; Schmahmann, 1996; Thach, 1996), affection and visceral functions (Bradley et al., 1987; Haines et al., 1990; Nisimaru et al., 1991; Waldrop and Iwamoto, 1991). To exert these different functions, the cerebellar cortical output is directed, via the cerebellar nuclei (CN), onto a large number of different brain stem nuclei (see Voogd, 1995) as has been studied in different species [rat: (Chan-Palay, 1977; Faull, 1978; Faull and Carman, 1978; Voogd, 1995); cat: (Voogd, 1964); monkey: (Asanuma et al., 1983)].

The output profile of the cerebellum is organized according to a modular pattern (Voogd, 1964; Oscarsson, 1969; Tolbert et al., 1978; Buisseret-Delmas and Angaut, 1993). A module consists of one or more parasagittally arranged strips of Purkinje cells that project onto a specific subdivision of the CN, both of which receive information from a specific part of the contralateral inferior olive. These olivo-cortico-nuclear modules have been suggested to represent functional cerebellar units (Oscarsson, 1979; Ekerot et al., 1995). In this way, different modules are thought to be involved in different tasks (Godschalk et al., 1994; van der Steen et al., 1994). As such, it would be expected that the output of these modules will reflect this functional heterogeneity.

However, to our knowledge, a detailed and comprehensive anterograde tracer study of the nucleobulbar projections in the rat is not available. Reports by Faull (1978) and Faull and Carman (Faull and Carmen, 1978) provide profiles of the distribution of nucleo-fugal projections, based on lesions and subsequent degeneration of the axons of the superior cerebellar peduncle. Other investigations into the cerebellar nuclear efferents only concerned parts of these projections, such as the projections of the CN to the inferior olive (Ruigrok and Voogd, 1990), the red nucleus (Angaut et al., 1987; Daniel et al., 1987), the nucleus reticularis tegmenti pontis (Cicirata et al., 1982; Angaut et al., 1985a) or the thalamus (Haroian et al., 1981; Angaut et al., 1985b). Only for the output of the lateral cerebellar nucleus an overview of all brain stem projections based on radioactive methionine tracing has been provided by Chan-Palay (1977). A survey of some of the main brain stem targets of the interface between the medial and interposed cerebellar nuclei was recently given by Buisseret-Delmas and colleagues (1998).

This chapter aims to provide a comprehensive overview of the nucleo-fugal projections in the rat, resulting from anterograde tracer deposits in different parts of the CN, thereby verifying and complementing results from the previously mentioned studies.

*Corresponding author. Tel.: +31 10 408 7296; Fax: +31 10 408 9459; e-mail: ruigrok@anat.fgg.eur.nl

Materials and methods

In this overview, the results of thirteen anterograde tracer injections, all made in the CN of adult, purpose-bred, male Wistar rats, will be presented and discussed. They were carefully selected out of a batch of 85 cases. The iontophoretic tracer injections were made with a glass micropipette containing either *Phaseolus vulgaris* Leucoagglutinin (PhaL) or biotinylated dextran amine (BDA). Details of surgical and immunohistochemical procedures are detailed elsewhere (Ruigrok and Voogd, 1990; Teune et al., 1998).

Serially collected transverse sections were analysed with a microscope equipped with a Lucivid™ miniature monitor and Neurolucida™ software. Contours, brain stem nuclei and main fiber tracts of equally spaced sections (spacing 320 μm of levels rostral to the decussation of the superior cerebellar peduncle and 640 μm of levels caudal to this point) were plotted at low magnification (objective 2.5 ×). Subsequently, at high magnification (objective 20 ×), the sections were systematically scanned and the positions of all labeled varicosities were digitized by mouse clicks. Varicosities in both PhaL and BDA labeled fibers have been shown to reflect synaptic boutons (Wouterlood and Groenewegen, 1985; Wouterlood and Jorritsma-Byham, 1993) and thus represent the most likely sites where information is transmitted to postsynaptic structures. In this way, for every plotted section, both the positions and number of plotted terminals was determined with reasonable accuracy. Only in areas with a very dense labeling such as occurring in the CN projections to the inferior olive or red nucleus is it likely that the number of plotted terminals represents an underestimate of the actual number of labeled varicosities. The number of plotted varicosities and the analysed surface area of the section were used to design a bulbar projection profile of a particular case. This profile indicates the relative amount of labeling along the rostrocaudal axis of the brain stem. Table 1, representing a survey of the results of all presented cases, was based on the computerized plots as well as on a supplement of the actual sections.

Nomenclature of brain stem structures is mostly based on Paxinos and Watson (1986). For the nomenclature and the subdivision of the red nucleus and the medial region of the mesodiencephalic junction we have followed Ruigrok and Cella (1995). The nomenclature will be further considered in the discussion. Delineation of the rat CN is slightly modified after Korneliussen (1968; see also: Ruigrok and Voogd, 1990; Buisseret-Delmas and Angaut, 1993; Voogd, 1995).

Results

For easy reference and comparison between selected cases, the location of the injection sites was indicated in standardized transverse drawings of the CN (Fig. 1). Both BDA and PhaL injection sites appeared as rounded, well-defined deposits of tracer substance from which labeled fiber bundles emerged. Within the brain stem these fiber bundles collateralized and showed terminal arborizations which carried many varicosities. The location of the varicosities was indicated in the plots. In accordance with a report on the similarity of BDA and PhaL-tracing (Wouterlood and Jorritsma-Byham, 1993), we noted no obvious differences in staining characteristics. However, based on the amount of labeled varicosities, BDA usually resulted in a smaller number of labeled terminal structures which most likely is related to the somewhat smaller appearance of the injection site. The results presented below will be illustrated with serial plots of actual sections and with the projection profiles which indicate the rostrocaudal levels of the brain stem that receive most prominent projections. An overview of the bulbar projections of all analysed cases is shown in Table 1.

Bulbar projections from the medial cerebellar nucleus

Three cases were selected with injections that were confined to various parts of the medial cerebellar nucleus (MCN: Fig. 1). The injection in case T195 (BDA) was restricted to its rostral half whereas case R100 (PhaL) centered on the caudal part of the nucleus. In an additional case (R127: PhaL) the injection was placed in the lateral aspect of the dorsolateral protuberance (DLP). Together, these cases provide an impression of the targets of the entire nucleus.

TABLE 1

Overview of all described cases indicating in which brain stem regions labeled varicosities were found. Large dot denotes dense labeling, small dot indicates only a minor projection, intermediate dot represents a fair projection. Question mark indicated that the area was not available for analysis; i indicates that the labeling was found ipsilateral to the injection site, otherwise the labeling was observed contralaterally

	MCN			PIN			AIN		DLH	LCN			
	T195	R127	R100	T82	T79	T108	R89	R98	R138	T77	T98	R178	T94
Medulla oblongata													
Inferior olive	•	●	●	●	●	●	●	●	●/●i	●	●/•i	●/•i	●/•i
Lateral reticular nucl.			•	•			•i	•i					
Nucl. of the solitary tract							•i						
Parasolitary nucl.	●/•i	●	●										
Medullary reticular nucl.	●/●i	•	•	•				•i	●i				
Paramedian nucl.				•									
Parvocell. retic. nucl.		•			•		•i	●i	•/●i	●/●i			●i
Gigantocell. retic. nucl.	●/●i	●	●	●						•	•		●/•i
Lat. paragigantocell. nucl.	●			•									●/•i
Spinal trigem. nucl., oral part		•					•i	•i	●i	●/●i			•i
Spinal trigem. nucl., interpolar part		•					•i	●i	●i	●i			•i
Spinal trigem. nucl., caudal part								•i	●i	•i			•i
Superior vestibular nucl.	•/●i	•/●i	•/•i	•i									
Lateral vestibular nucl.	•/●i		•/•i	•i			•i	•i			•i		
Medial vestibular nucl., rostral	•/•i	•i	•/•i	•i							•i		
Medial vestibular nucl., caudal	•/•i		•/•i	•i									
Spinal vestibular nucl.	●/●i	•	•/•i	●i			•i		•i				
Nucl. prepositus hypoglossi			●/•i										
Metencephalon													
Basal pontine nuclei			•				•	•	●		●	●	●
Nucl. retic. tegm. pontis		•	●	●	•		●	●	●	●	●	●	●
A5 noradrenergic group (?)		•	•	●				•i	●i	●i			•i
Principal sens. trig. nucl.		•							•				
Caud. pont retic. nucl.	●	●	●	●			•			•		•	●/•i
Oral pont. retic. nucl.	•	●	●	•			●			•	•	●/•i	●/•i
Central gray pons		•	●/•i		•							●	●
Pedunculopontine tegm. nucl.		●	●		•		•			•i	•i	●	•
Parabrachial nucl.		●/•i	•/•i						•i	•i	•i		
Mesencephalon													
Red nucl., parvicellular	•		•	•	•		•	•	•	●	●	●	●
Red nucl., magnocellular	•			•	●		●	●/•i	●	•	●		
Pararubral area		•	●									●	●
Deep mesenceph. nucl.		●	●	●	•	●	•	●	●	●	•	●	●
Superior colliculus, superficial												●	
Superior colliculus, intermediate			•			●		•				●	•
Superior colliculus, deep		●	●			●	•	•				●/•i	●
Ventral tegmental area			•										
Dorsal raphe nucleus			•							•i			•
Ventral tegm. relay zone			•		●				●	●	•	•	●
Medial access. oculomot. nucl.		•	●								●	●/•i	●/•i
Interstitial nucl. of Cajal	●	●	●	•	•	•					•	•	●/•i
Nucl. of Darkschewitsch			●								•	●	•
Nucl. parafascicularis prerubr.	●	•	●	●	●	●	●	•	•	●	●	●	●/•i
Periaquaductal gray		●	●		•	•	•					●	●
Nucl. of post. commissure			●			●		●				●	●/•i
Anterior pretectal nucl.			•				●	●	•	●	●	●/•i	●
Posterior pretectal nucl.							•	•		●	•	●/•i	•

TABLE I—Continued

	MCN			PIN			AIN		DLH	LCN			
	T195	R127	R100	T82	T79	T108	R89	R98	R138	T77	T98	R178	T94
Diencephalon													
Mammillary nuclei												•	
Lateral hypothal. area			•									●/•i	•
Dorsal hypothal. area			•									●/•i	•
Zona incerta			•	•	•	●	●	●		•	●	●/•i	●/•i
Nucl. fields of Forel	•	•	●	●	•	•	•	•	•	●	●	●/•i	●/•i
Ventral lat. geniculate nucl.						•						•	•
Parafascicular thalam. nucl.		●	●	•			●	•			•	●/•i	●
Central medial thalam. nucl.		•						•	•		•		•
Laterodorsal thalam. nucl.						•	•	•				●	•
Posterior thalamic nucl.		•		•		●	•	•	●	●	•		•
Ventroposterior thalam. group		•				•	•						•
Ventromedial thalam. nucl.	•	●	●	•	•	•	•	•		•	•	●	●/•i
Ventrolateral thalam. nucl.	•	?	?	●	?	●	●	●		●?	●	?	●

Case T195

From the plots of this case (Fig. 2) as well as from the projection profile shown in Fig. 8, it is obvious that most labeling was found in the caudal part of the brain stem. The labeling in the inferior olive (IO) was restricted to the caudolateral part of the medial accessory olive (MAO: not shown in Fig. 2) and subnucleus β contained a few labeled terminals. Main brain stem targets were the vestibular nuclei. In particular, the superior (SVN), lateral (LVN) and spinal (SpVN), and the rostral, magnocellular parts of the medial vestibular nucleus (MVN) were heavily labeled. Within the SVN, MVN and LVN, most labeling was found at the ipsilateral side, whereas the labeling in the SpVN was predominantly observed contralateral to the injected side. The latter labeling extended caudalwards into the parasolitary region. Within the reticular formation, both the ipsilateral and contralateral medullary reticular nuclei and the gigantocellular reticular nucleus (Gi) showed some bilateral terminal labeling. Some sparse labeling was noted in the ipsilateral lateral reticular nucleus (LRN). However, within the pontine reticular formation labeling was restricted to the contralateral side. Some labeling was noted within and directly below the locus coeruleus of both sides (Fig. 2: level 10). The mesencephalon contained little labeling; some labeled terminals were found in the lateral horn of the magnocellular red nucleus (level 8). Within the medial mesodiencephalic region varicosities were noted in the interstitial nucleus of Cajal (INC) and in the area surrounding the fasciculus retroflexus (fr), such as the prerubral field, the rostral interstitial nucleus, the subparafascicular nucleus, and which have been collectively termed the area parafascicularis prerubralis by Carlton et al. (1982). Within the diencephalon, some labeling was noted ventrally in the ventromedial (VM) and laterally in the ventrolateral (VL) thalamic nuclei.

Case R127

In case R127, PhaL had been injected into the lateral aspect of the DLP region of the MCN (Fig. 1). Plots, shown in Fig. 3, as well as the projection profile (Fig. 8) indicate that, compared to T195, a considerable part of the projection from this area is directed to more rostral brain stem areas.

In the IO, terminal labeling was found medially in the caudal MAO, but not in the adjacent subnucleus β. Although some labeling was observed in the caudal part of the contralateral reticular formation, most labeling was noted at more rostral levels. Labeling was especially dense over the parvicellular reticular nucleus (PCRt) but was also distributed to the dorsolateral Gi, as well as to the caudal (PnC) and oral (PnO) parts of the pontine reticular nuclei and extending into the pedunculopontine tegmental nucleus. Relatively few terminals were found in the vestibular complex; only the SVN and the SpVN contained some labeled varicosities. The ipsilateral projection to the

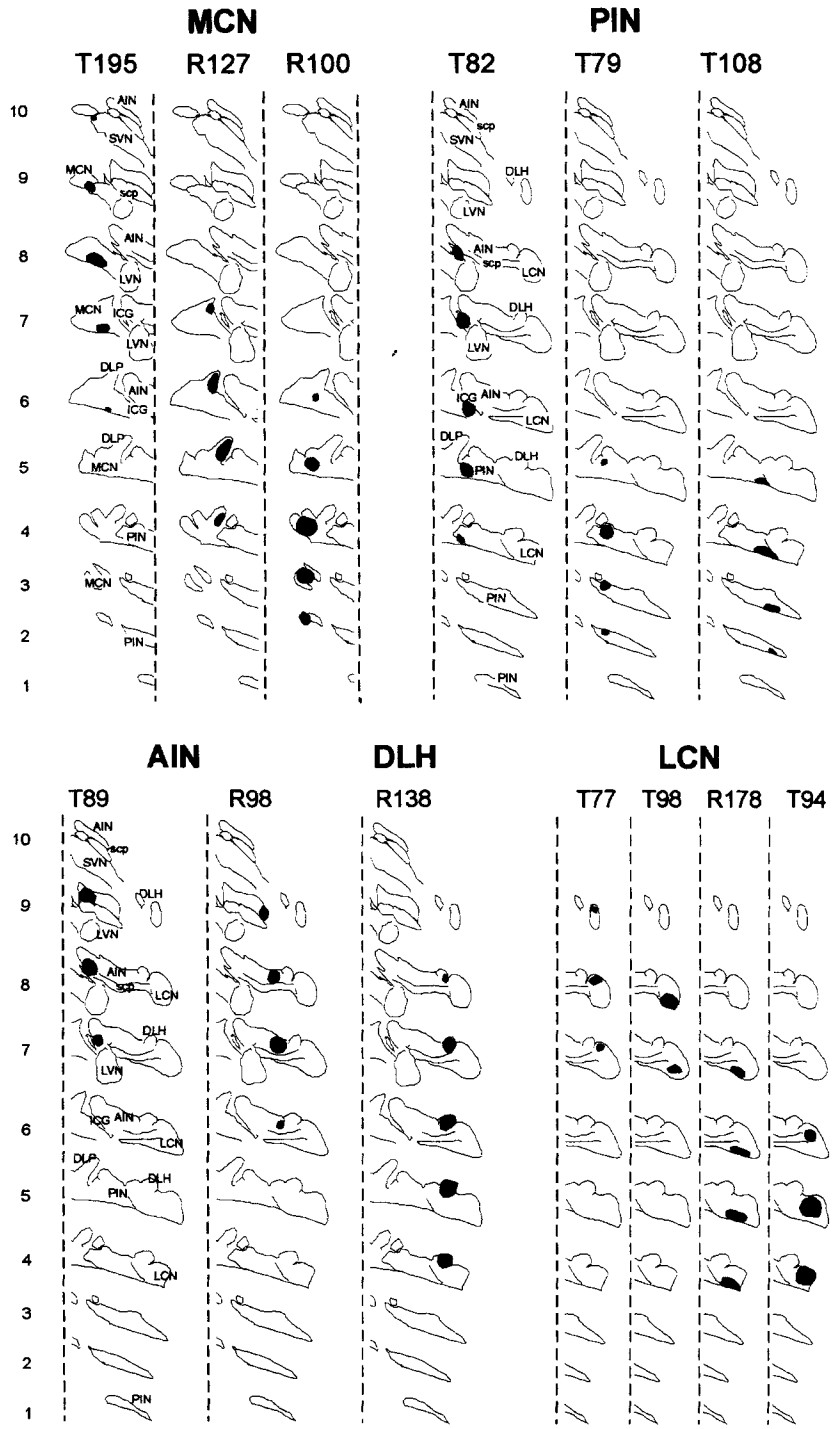

Fig. 1. Diagrams of the injection sites described in this paper. The injection sites are indicated in a standardized, equally spaced (160 μm), series of transverse sections displayed from caudal (1) to rostral (10). For abbreviations, see List.

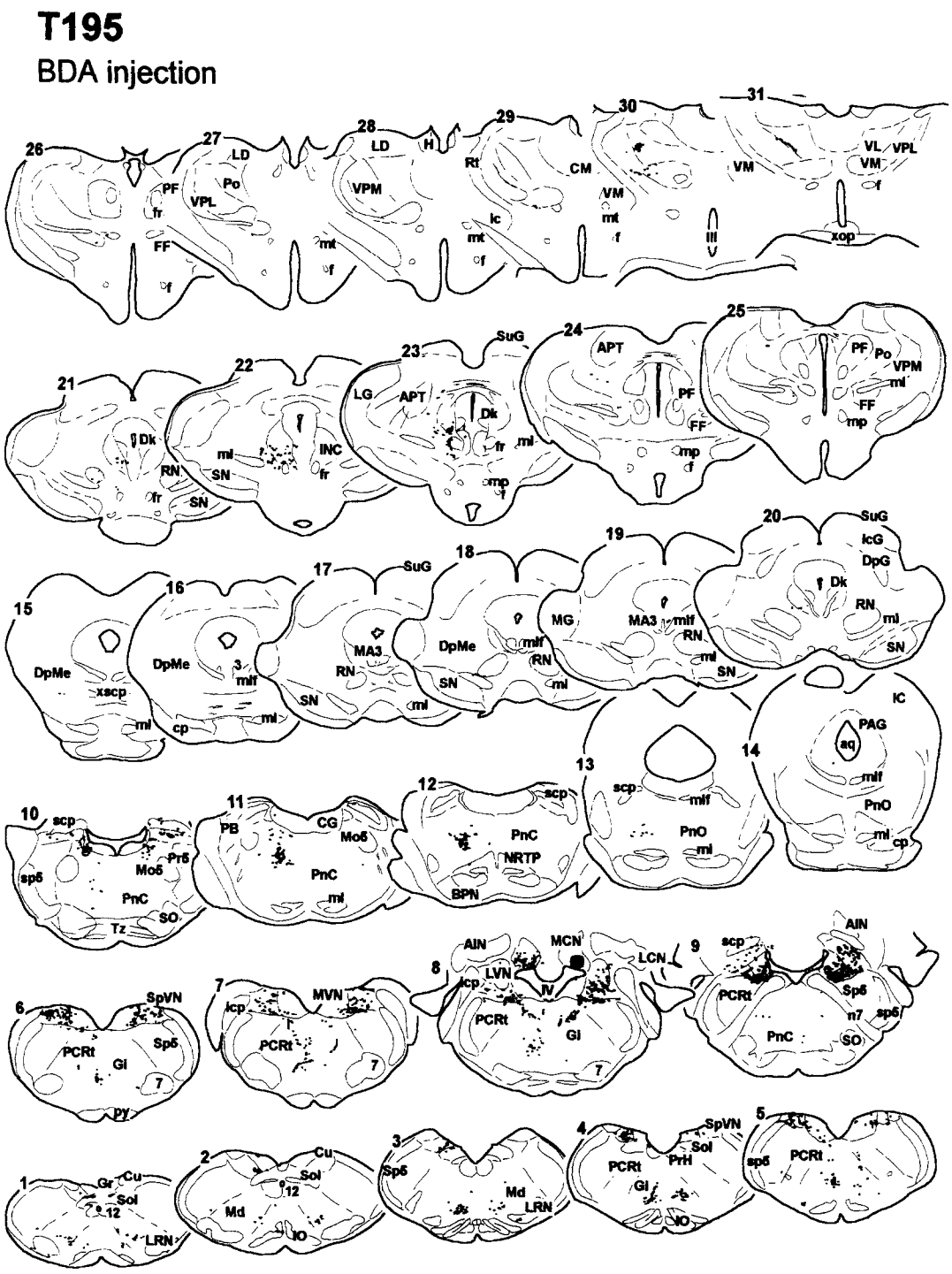

Fig. 2. Serial plots indicating the distribution of labeled varicosities (dots) throughout the brain stem in case T195 with a BDA injection centered on the rostral part of the MCN. For details of the injections site, see Fig. 1. The boundaries of several brain stem nuclei (hatched lines) and fiber tracts (thin lines) are indicated. For abbreviations, see List.

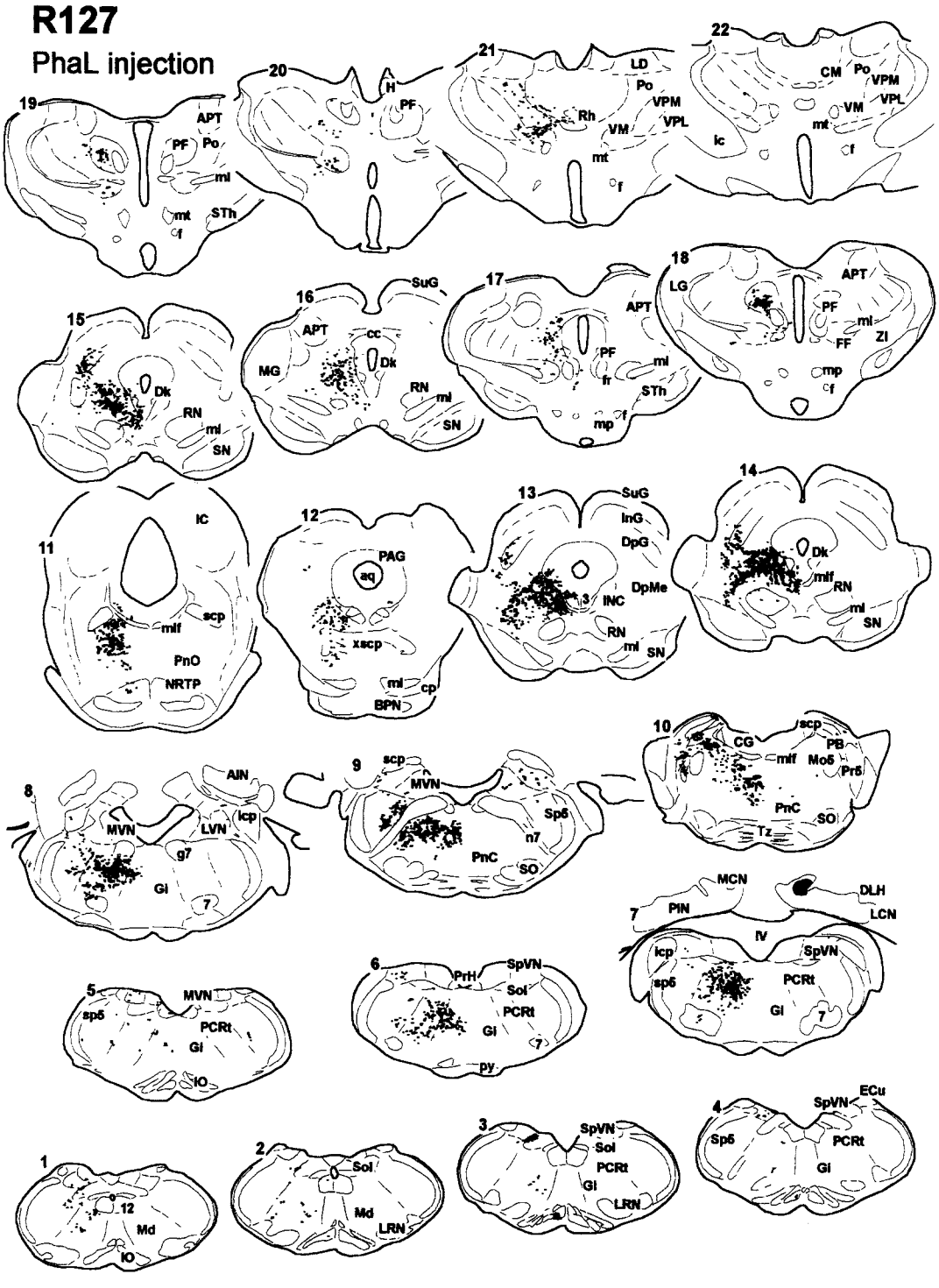

Fig. 3. Serial plots showing the distribution of labeled varicosities in case R127 with a PhaL injection centered on the DLP. Further as in Fig. 2.

SVN predominated over the contralateral projection. The deeper parts of the contralateral spinal trigeminal nucleus (the pars caudalis, the pars interpolaris and, to a lesser extent, the pars oralis) also were provided with input. In addition some labeling was found in the nucleus reticularis tegmenti pontis (NRTP).

A small but significant projection to the parabrachial nuclei (PB) was found, ipsi- as well as contralateral to the injection site, with the contralateral projection predominating. In the midbrain, labeling was only noted contralateral to the injection site. The deep mesencephalic nuclei (DpMe) received a strong projection, however, the red nucleus (RN) remained devoid of labeling. Heavy labeling was observed in the INC. Several additional regions such as the medial accessory oculomotor nucleus (MA3), the nucleus of the posterior commissure, and the prerubral region contained labeled terminals. In addition, varicosities were noted in the deep layers of the superior colliculus (SC). In the diencephalon, terminals filled with PhaL were found in several nuclei such as the parafascicular nucleus (PF), the central medial nucleus (CM) as well as in the VM, VL and posterior thalamic nuclear group (Po).

Case R100

In this case, the injection of PhaL was centered on the caudal aspect of the MCN, but without incorporation of the DLP (Fig. 1). This particular case demonstrated a large yield of labeled varicosities which was distributed over the entire length of the investigated part of the brain stem (Figs 4 and 8).

Within the contralateral IO, labeled terminals were observed in the lateral-most aspect of the caudal MAO as well as in the ventromedial part of subnucleus β and possibly converging on the medial aspect of subnucleus *c* (Akaike, 1992). From the plots of Fig. 4 it is obvious that most prominent labeling was found in the medial part of the contralateral reticular formation at the rostral medullar and pontine levels. In the medullar reticular formation, labeling was mostly restricted to the dorsal part of the Gi where it appeared to be continuous with labeling in the nucleus prepositus hypoglossi (PrH). Labeling within the PnC was continuous with dense projections to the pontine central gray. Some ipsilateral projections to these areas were also noted. Labeling was virtually absent in the PCRt and spinal trigeminal complex. Relatively sparse labeling was observed in the vestibular complex on both sides of the brain. A conspicuous projection to the contralateral parasolitary nucleus was in accordance with other cases of this series. The PB and pedunculopontine tegmental nucleus received a mostly bilateral projection. Labeled fibers carrying varicosities furthermore reached dorsal and medial aspects of the NRTP and basal pontine nuclei (BPN). The mesencephalon also contained numerous labeled terminals, mainly distributed to the contralateral DpMe, MA3 and periaquaductal gray (PAG). Both the magnocellular and the parvicellular RN contained only a few labeled terminals. More dense terminal labeling was observed in the pararubral and prerubral regions, including the nucleus of Darkschewitsch (Dk), the area surrounding the fr, and the nucleus of the posterior commissure. In addition, labeling was noted in the deep and intermediate layers of the SC and extending into the pretectal regions. Ventral to the RN, some terminals reached into the ventral tegmental area. The thalamus contained terminals in the VM, and in the intralaminar nuclei, with most abundant labeling in the PF. Additional labeling was observed in the fields of Forel (FF) which extended into the dorsomedial part of the zona incerta (ZI). In this series of MCN injections, this was the only case that demonstrated terminal labeling that reached the dorsal aspects of the hypothalamus.

Projections from the posterior interposed nucleus and the interstitial cell groups

Three injections were selected to characterize the projections from the posterior interposed nucleus (PIN). Selection of these cases was mainly based on differences in the mediolateral position of the injection site. The most rostromedially placed injection (T82) involved the so-called interstitial cell groups (ICG) which are interspersed between the MCN and both interposed nuclei (Buisseret-Delmas et al., 1993). The injections in cases T79

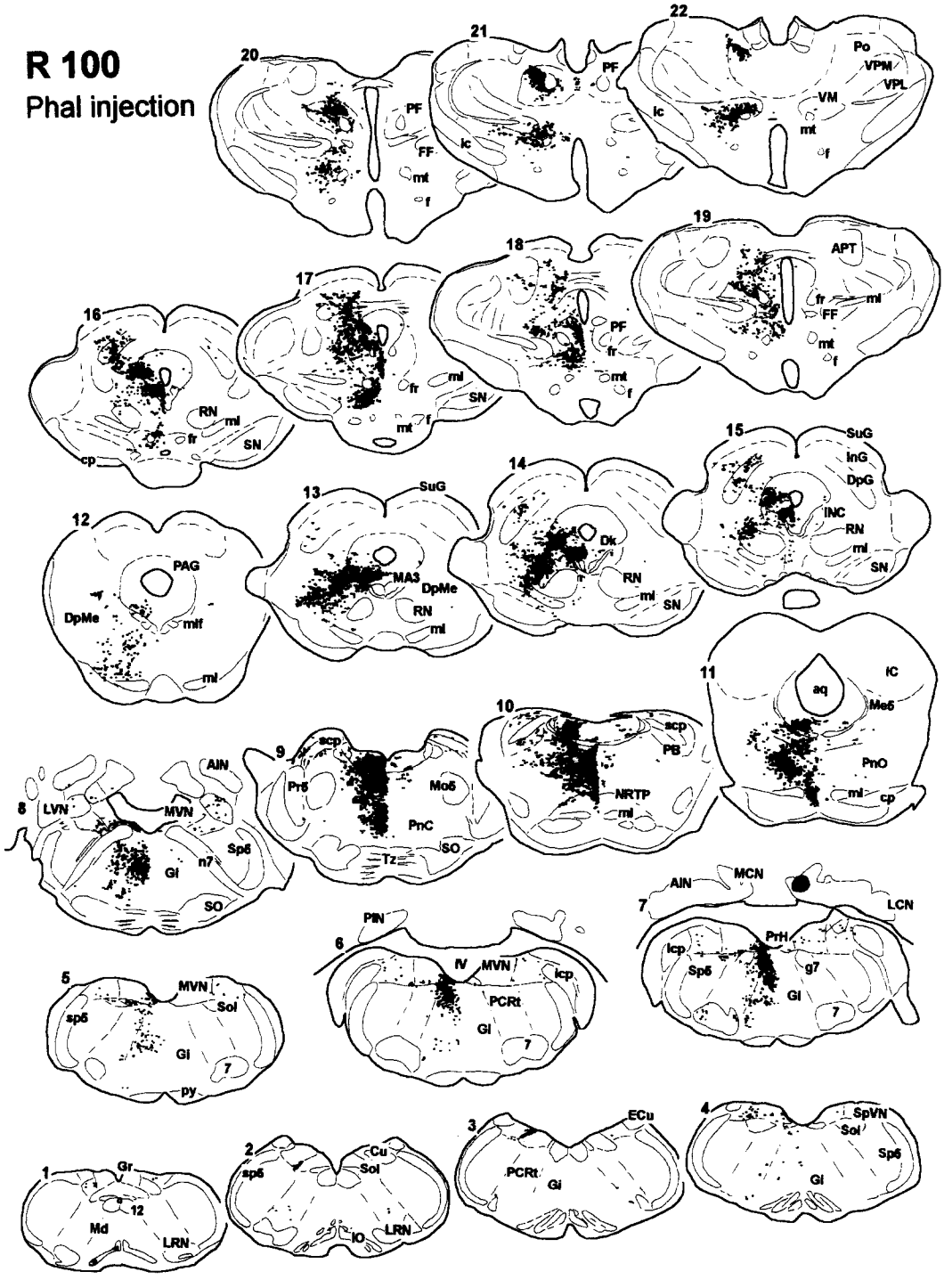

Fig. 4. Serial plots showing the distribution of labeled varicosities in case R100 with a PhaL injection centered on the MCN. Further as in Fig. 2.

and T108 were placed at progressively more lateral levels but remained confined within the boundaries of the PIN (Fig. 1).

Case T82

In this case the BDA injection was centered on the ICG, without any obvious involvement of either the MCN or the anterior interposed nucleus (AIN: Fig. 1). This could be ascertained by the fact that virtually no terminal labeling was observed in the dorsal accessory olive (DAO), indicating that the medial AIN was not involved in the injection site (Ruigrok and Voogd, 1990; Buisseret-Delmas et al., 1998). As shown in the plots of Fig. 5 and in the projection profile of Fig. 8, the projection pattern was more or less equally dispersed over virtually the whole length of brain stem. The only clear concentration of terminals was found in the lateral half of the central MAO. Further medullary labeling was noted in the contralateral Gi and paragigantocellular nucleus and in the ipsilateral vestibular nuclei which did not extend into the parasolitary nuclei. Some labeling was also noted in the NRTP and pontine reticular formation. In the mesencephalon projections were noted to the DpMe, the INC and the prerubral region. In the RN, especially its magnocellular and to a lesser extent its parvicellular part, displayed labeled varicosities that were mostly concentrated along the ventromedial contour of the nucleus. The ventral part of the ZI displayed several labeled terminals as did the PF. More pronounced labeling was noted in the FF, the VM, the Po, and scattered throughout the VL.

Projections originating from the ICG and terminating in the caudoventral RN, the dorsal NRTP, the INC, the vestibular nuclei (especially ipsilaterally) and the IO have recently been described by Buisseret-Delmas et al. (1998). Since the spinal cord was not investigated in this study, the potentially important projections from this area to the cervical cord could not be verified (Horn et al., 1995).

Case T79

BDA had been injected medially in the more rostral parts of the PIN without obvious involvement of either the ICG or AIN. When compared to the former case, the resulting projections may be characterized by the relative lack of labeling in the caudal brain stem (Figs 6 and 8). Olivary labeling was noted caudally in the rostral half of the MAO, at a level somewhat more rostral than in case T82. In the medulla, besides the olivary labeling, only some varicosities were distributed to the contralateral PCRt. A more pronounced labeling was noted in the medial margin of the magnocellular RN. Additional projections were noted to the DpMe, the visual tegmental relay zone (VTRZ) and to part of the nucleus parafascicularis prerubralis located just dorsal to the fr (level 16 of Fig. 6). Unfortunately, rostral thalamic levels were not available for analysis.

Case T108

The injection site (BDA) in T108 was centered on the lateral aspect of the PIN (Fig. 1). In the IO, a dense patch of terminal labeling was found medially in the rostral-most tip of the MAO. Other medullary regions remained devoid of labeling (Figs 7 and 8). A large part of the projections were directed to the SC where especially the deep and intermediate levels contained many labeled varicosities. Projections also reached the DpMe, the INC, the PAG, the nucleus of the posterior commissure, the Dk and, more sparsely, the prerubral area surrounding the fr. The RN was virtually devoid of labeled varicosities. A considerable projection was directed to the ZI, part of the labeling extended into the ventral lateral geniculate nucleus. In the thalamus, further terminal labeling was found in the VM and in the dorsomedial part of the VL.

Projections from the anterior interposed nucleus and dorsolateral hump

In order to describe the bulbar projections from the AIN, a medially (R89) and a laterally (R98) placed injection will be presented together with an injection that was centered on the dorsolateral hump (DLH: R138)). This part of the CN consists of a conspicuous neuronal mass which protrudes somewhat between the lateral parts of the interposed

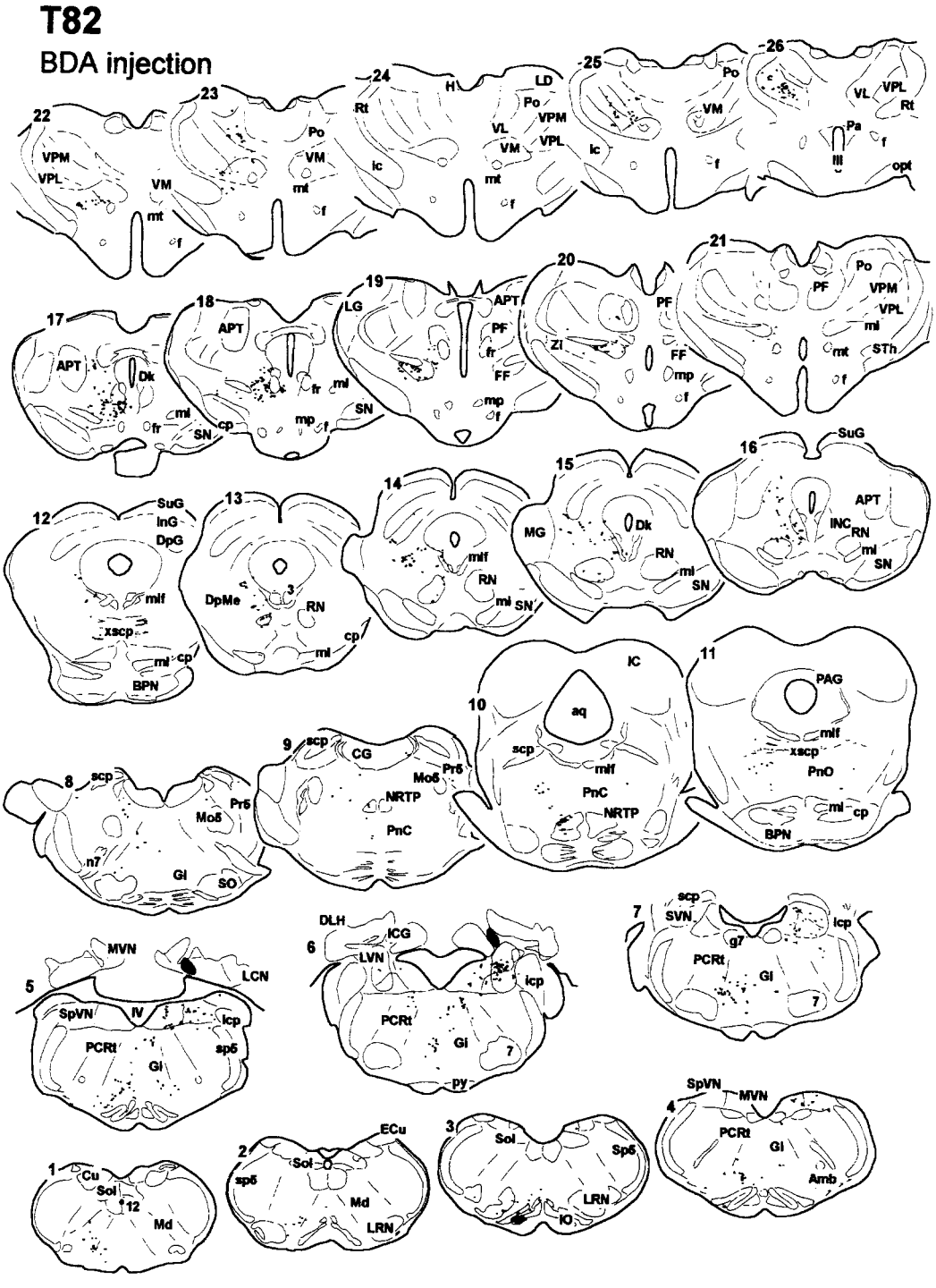

Fig. 5. Serial plots showing the distribution of labeled varicosities in case R82 with a BDA injection centered on the ICG. Further as in Fig. 2.

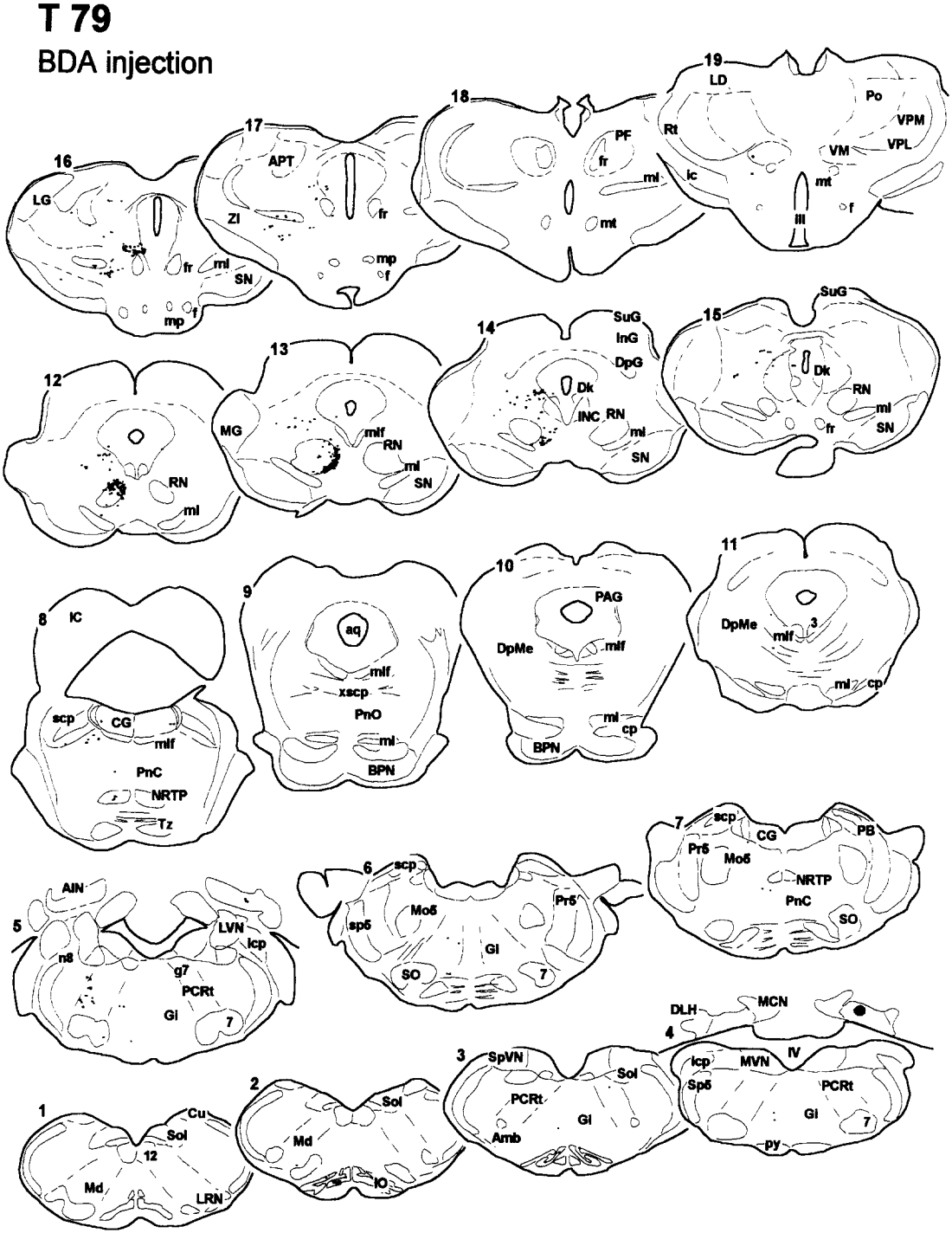

Fig. 6. Serial plots showing the distribution of labeled varicosities in case T79 with a BDA injection centered on the medial aspect of the PIN. Further as in Fig. 2.

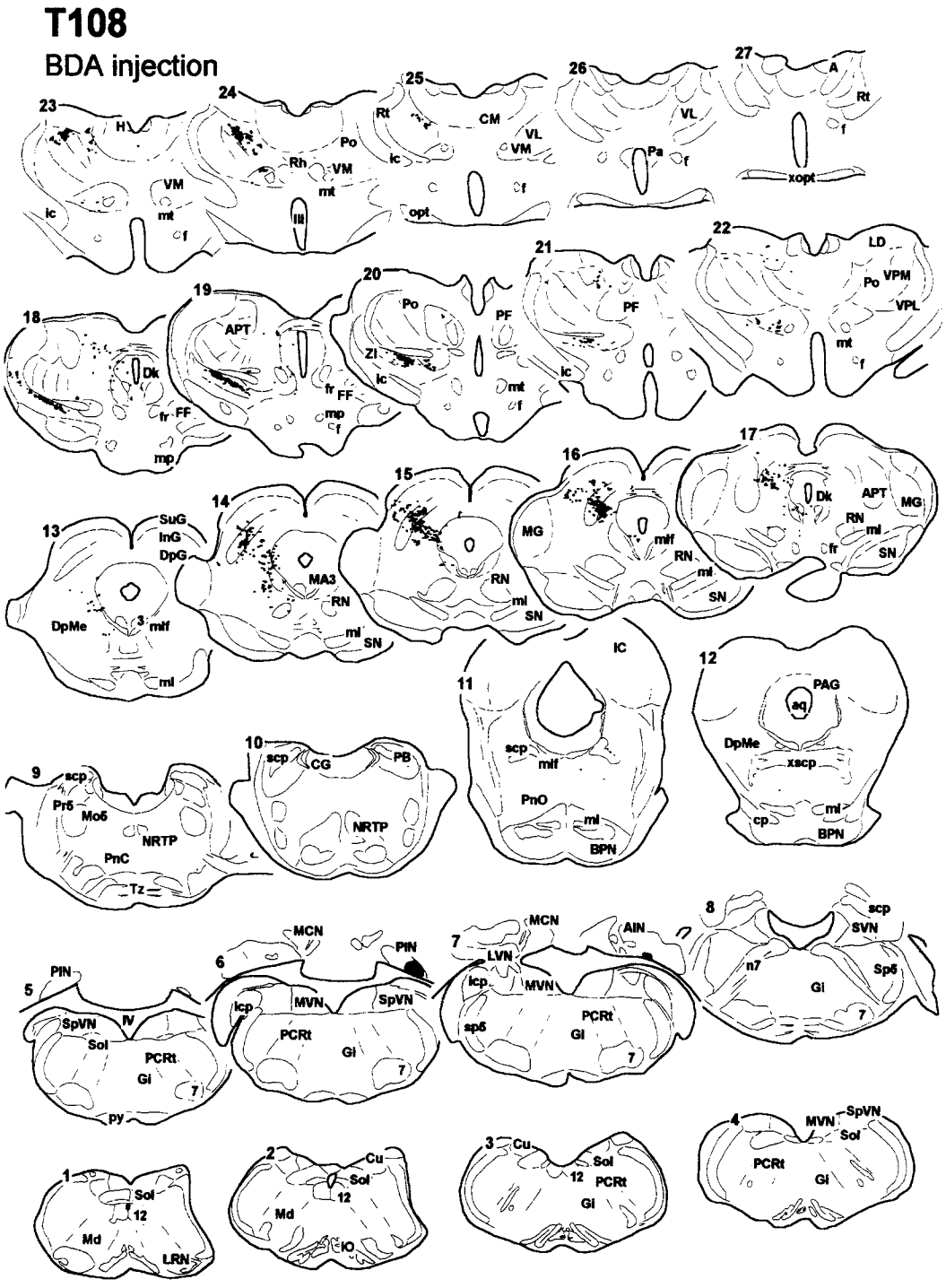

Fig. 7. Serial plots showing the distribution of labeled varicosities in case T108 with a BDA injection centered on the lateral aspect of the PIN. Further as in Fig. 2.

nuclei and the dorsomedial part of the lateral cerebellar nucleus (Korneliussen, 1968).

Case R89

In this case the PhaL injection was confined to the medial part of the rostral half of the AIN (Figs 1 and 9). Although most fibers were directed to the contralateral ascending pathway, some scattered labeled varicosities were found in the ipsilateral vestibular nuclei, particularly within the SpVN, in the PCRt and, sparsely, within the spinal trigeminal complex. An abundant projection, in addition, was noted to the lateral part of the caudal DAO. At pontine levels, the contralateral NRTP and BPN contained labeled terminals. More distributed varicosities were noted in the PnO and pedunculopontine tegmental nucleus. The ventral

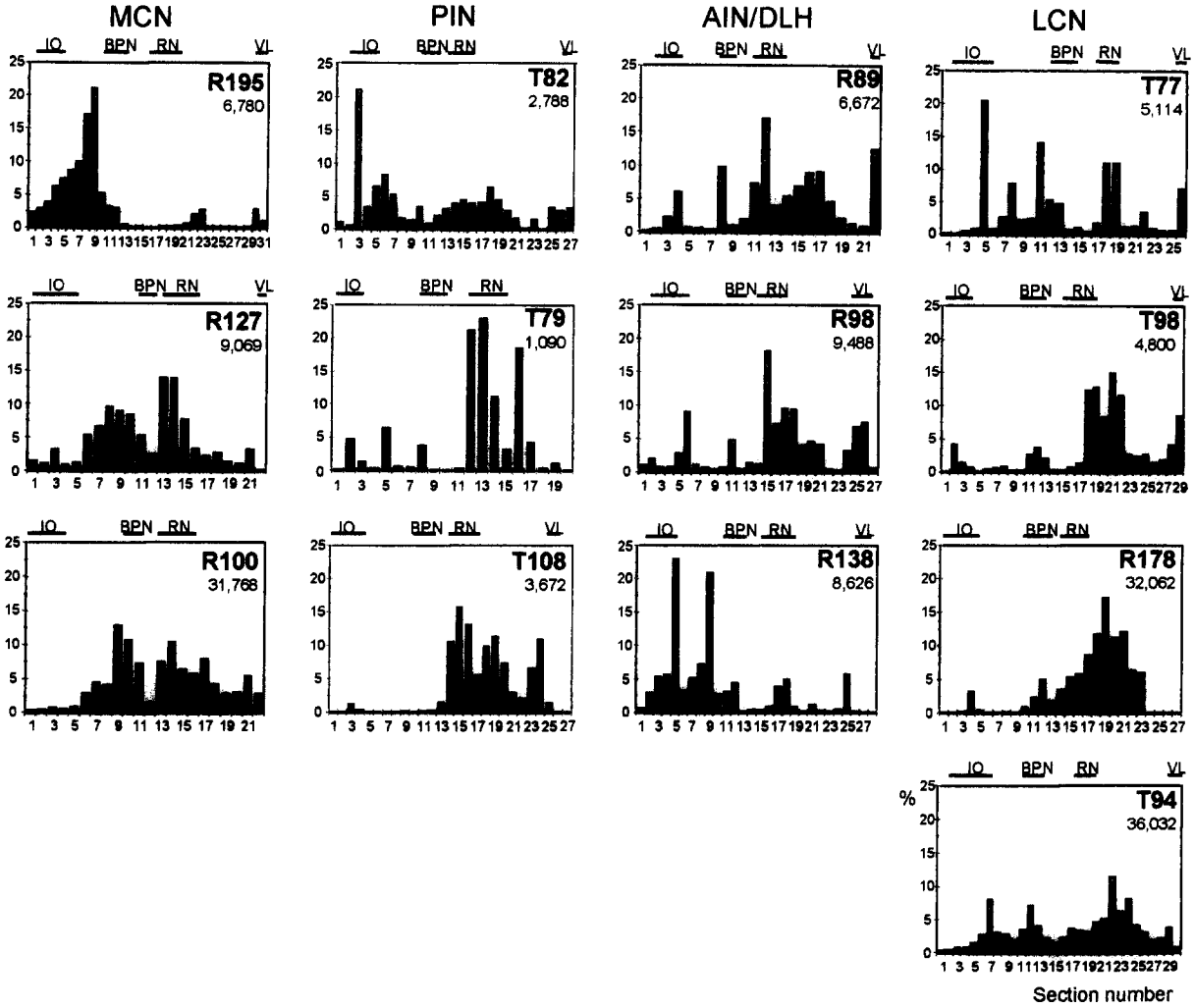

Fig. 8. Bar diagrams indicating rostrocaudal distribution of labeled varicosities of thirteen cases shown in Figs 2–7 and 9–15. The x-axis displays the section number of the corresponding plots (Figs 2.3 to 2.7). The Y-axis displays the percentage of plotted varicosities. The total number of plotted varicosities is indicated below the case number. The approximate rostrocaudal position of four brain stem areas (IO: inferior olive; BPN, basilar pontine nuclei; RN: red nucleus; and VL: ventrolateral thalamic nucleus) is indicated above each graph for easy reference. Note that cases R195 and R199 mostly projects to the caudal brain stem levels whereas cases that involve the DLP and especially the caudal MCN (R100) in addition or rather (R100) supply more rostral brain stem areas.

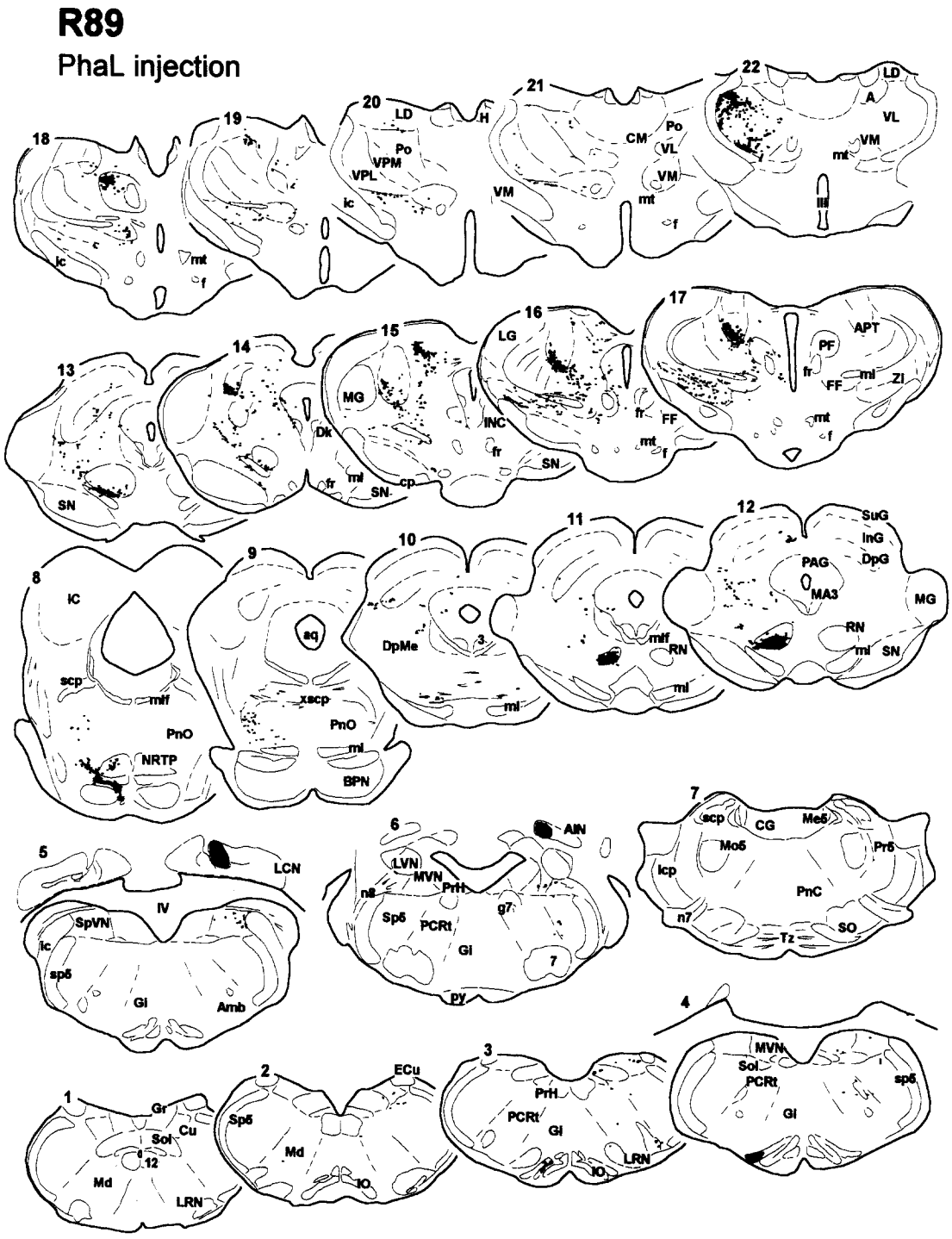

Fig. 9. Serial plots showing the distribution of labeled varicosities in case R89 with a PhaL injection centered on the medial aspect of the AIN. Further as Fig. 2.

part of the contralateral magnocellular RN contained a dense cluster of labeled terminals which extended somewhat into the parvicellular part of the nucleus. Projections were furthermore noted to the DpMe, the SC, the prerubral area, and the PAG; the labeling to the DpMe extended into the ventral part of the anterior pretectal nucleus (APT) where a significant projection was observed; in addition, labeling was noted in the posterior pretectal nucleus. In the diencephalon, both the dorsal and ventral parts of the ZI contained a fair amount of terminals. Furthermore, terminal labeling was observed in the PF, VM, VL, and laterodorsal thalamic cell groups (LD). Within the VL most labeling was found at the periphery of the nucleus.

Case R98

Case R98 was characterized by a PhaL injection that was centered on the lateral part of the AIN, however without involving the DLH (Fig. 1). Plots and projection profile are shown in Figs 10 and 8, respectively. The olivary labeling in this case, contrasting with case T89, was characterized by an impressive number of labeled terminals that were located in the mediorostral part of the DAO. Furthermore, the ipsilateral medulla oblongata, in particular the PCRt and the deep layers of the entire spinal trigeminal nucleus, received a substantial projection from the lateral AIN. Some labeling extended into the subtrigeminal part of the LRN; also, varicosities were noted ventrally in the LVN. At pontine levels, more abundant projections were noted especially to the contralateral NRTP and, to a lesser extent, the BPN. Also, some terminals were observed in the approximate location of the ipsilateral A5 noradrenergic group (Fig. 10, level 10: see also projections that originate from the lateral cerebellar nucleus). More rostrally, the dorsal half of the magnocellular RN contained a dense cluster of labeled terminals, which extended somewhat into the parvicellular part of this nucleus. The DpMe, intermediate layers of the SC, and the prerubral area only received a minor projection; a very prominent projection, however, was noted to the pretectal area, especially to the APT. A mediolateral band of labeled varicosities was furthermore found in the ventral ZI. Most labeling in the thalamus was found in the VL and PF, although some varicosities were also noted in the Po, LD, and VM.

Case R138

The injection site in this experiment particularly involved the rostral part of the DLH, without obvious involvement of either the interposed or lateral cerebellar nuclei (Fig. 1). The IO showed labeling which was found bilaterally in the dorsomedial group (DM), which is usually considered a part of the principal olive (PO: e.g. Buisseret-Delmas and Angaut, 1993, however, see also Ruigrok and Voogd, 1990). From the projection profile (Fig. 8) it is obvious that in this case only a fraction of its connections was directed to levels rostral to the pons. Several structures in the medulla oblongata and metencephalon, ipsilateral to the injection site, contained numerous labeled terminals such as the medullary reticular nuclei (both ventral and dorsal subdivisions), the PCRt, and along the whole length of the spinal trigeminal nucleus. The projection to the PCRt also contained a small contralateral component. At pontine levels, many labeled varicosities were found interspersed between the principal and motor nuclei of the trigeminal complex (Fig. 11, level 10). Ventralwards these fibers appeared to reach the A5 noradrenergic cell group. Furthermore, pontine projections were noted contralaterally to the NRTP and the BPN and ipsilaterally to the PB. In the mesencephalon, both the magnocellular and the parvicellular parts of the RN contained a few labeled terminals, predominantly in their dorsal and dorsomedial aspects. Dorsal to the RN, some terminal labeling was found in the DpMe. In addition, labeling was noted in the VTRZ and in the prerubral area. At thalamic levels only sparse labeling was noted, medially in the Po and extending somewhat into the CM of the intralaminar nuclei. No projection to the VL was observed.

Projections from the lateral cerebellar nucleus

Four cases were selected to analyse the bulbar projections that originate from the lateral cerebellar

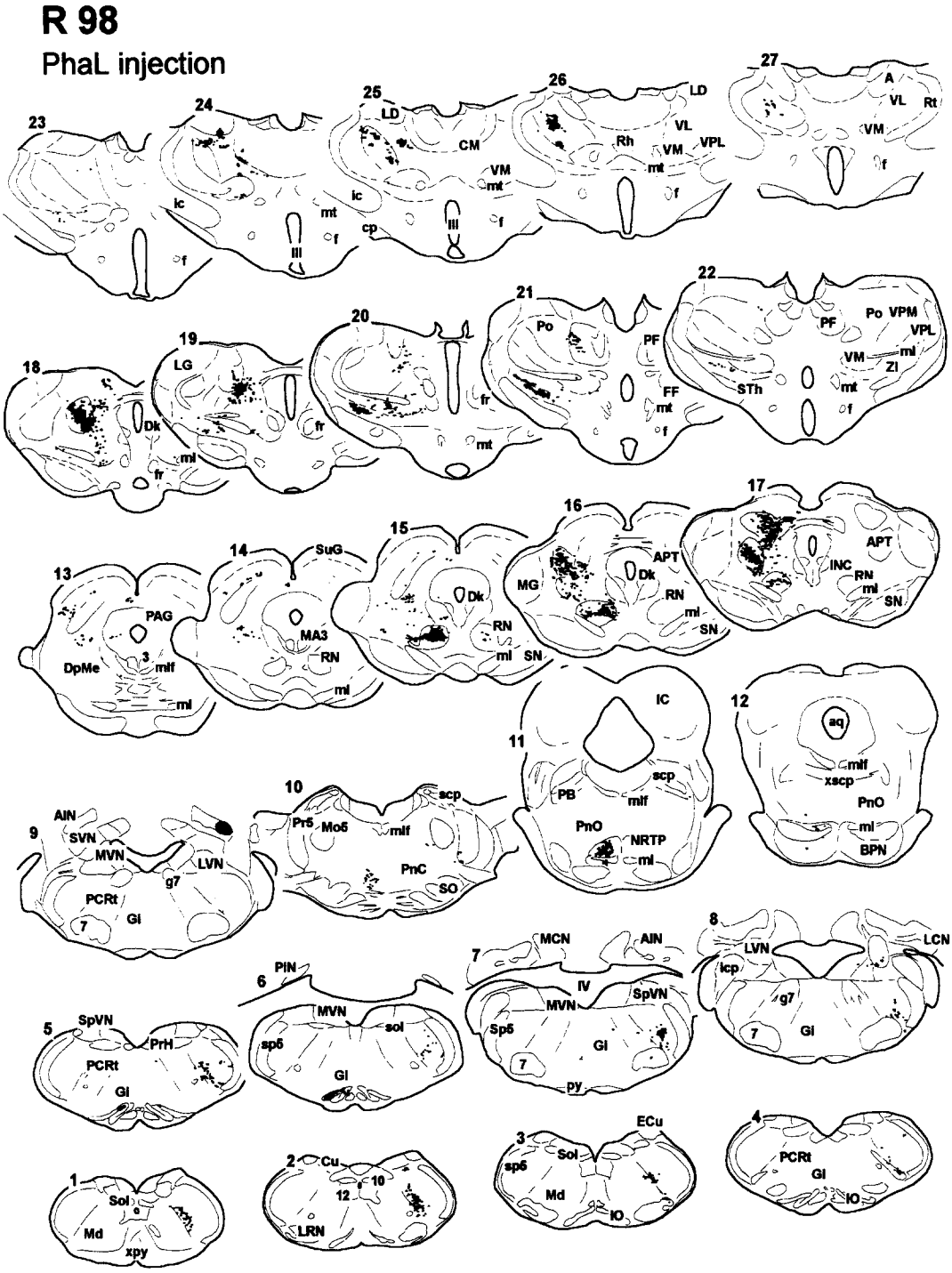

Fig. 10. Serial plots showing the distribution of labeled varicosities in case R98 with a PhaL injection centered on the lateral aspect of the AIN. Further as Fig. 2.

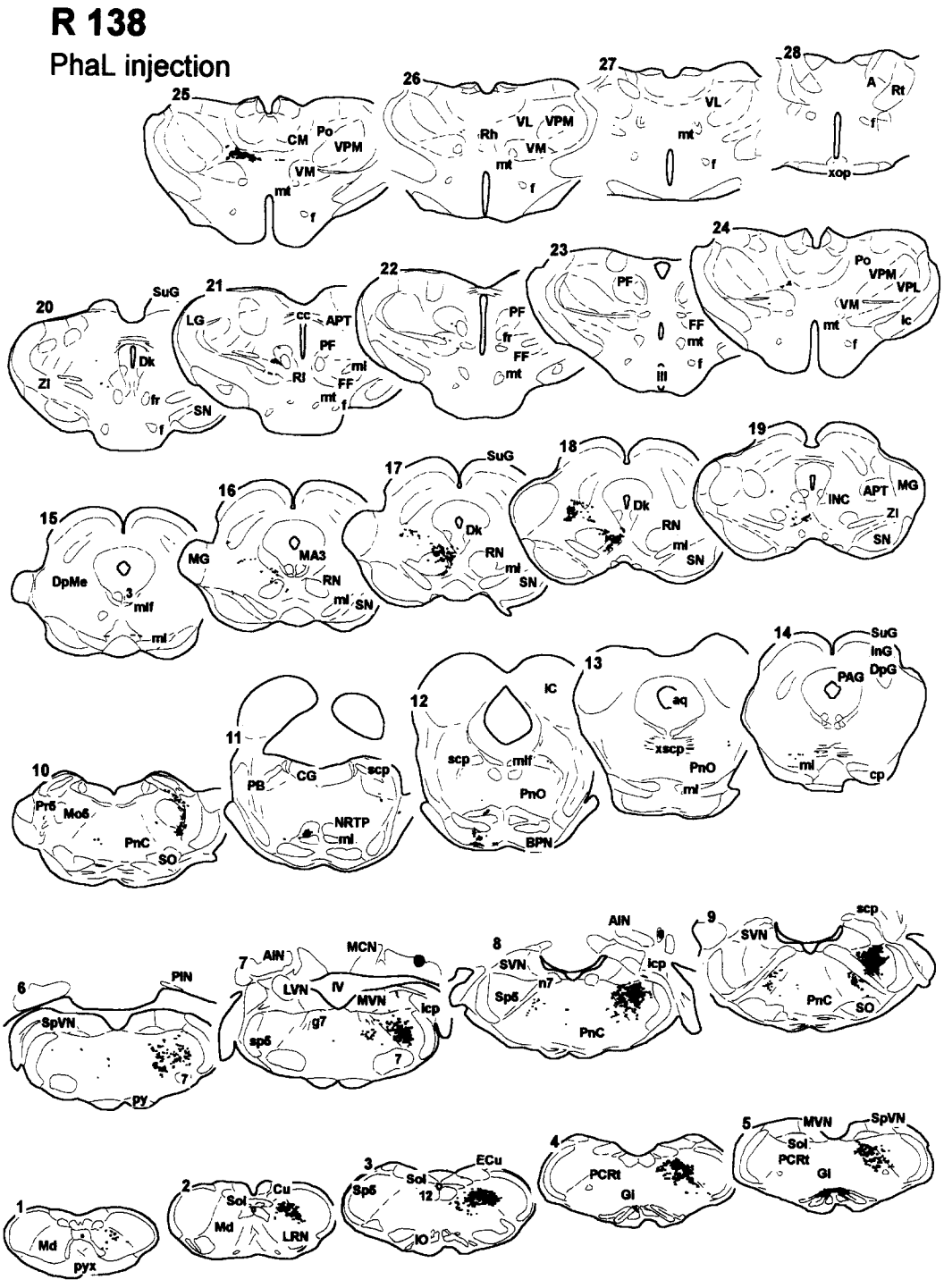

Fig. 11. Serial plots showing the distribution of labeled varicosities in case R138 with a PhaL injection centered on the DLH. Further as Fig. 2.

nucleus (LCN). Two injections were centered on the rostral aspects of the nucleus; one into its dorsal tip (T77) and one covering the ventral half (T98). The other cases were centered on the caudal half of the nucleus; R178 focusing on its ventral, parvicellular, part and T94 covering somewhat more dorsal aspects.

Case T77

In this case, a relatively small injection with PhaL was centered at the dorsal margin of the rostral half of the LCN, however, without involvement of the DLH (Fig. 1). This was corroborated by the observation that the olivary projection was restricted to the dorsal lamellae of the PO, without any labeling of the DM group (Fig. 12, level 5).

In the medulla oblongata, terminal labeling was distributed bilaterally. Apart from the olivary labeling, the most prominent projections were observed in the ipsilateral PCRt, which appeared reminiscent to the projections arising from lateral AIN and DLH, although they did not extend as far caudally. Labeled varicosities were also noted within the confines of the spinal trigeminal nucleus, especially within its oral part. At the pontine level a conspicuous input to the ipsilateral A5 area (Paxinos and Watson, 1986), located just ventral to the motor nucleus of the trigeminal complex (Fig. 12, level 10, 11) was also noted. Dense patches with varicosities were furthermore located within the contralateral NRTP. Some varicosities were noted in the dorsal raphe nucleus (Fig. 12, level 14).

In the mesencephalon, input was specifically noted to the DpMe and extending into the nucleus of the optic tract and caudal part of the APT. In the RN, most terminals were distributed within the dorsomedial aspect of its parvicellular part, extending somewhat into the VTRZ but more prominently into the prerubral region and FF. Within the ZI, only a few scattered varicosities were noted. Thalamic labeling was found in the VM and caudomedial VL. More rostral levels, however, were not available for analysis.

Case T98

Here, the injection (BDA) was centered on the ventral aspect of the rostral LCN (Fig. 1). Within the IO, most prominent labeling was confined to the caudal-most aspect of the PO (Fig. 13, level 2). From the projection profile (Fig. 8) it can be seen that the major part of the projection is directed to the mesodiencephalic transition area (levels 18–22 of Fig. 13). Within the medulla oblongata, only a few labeled terminals were found, mainly ipsilateral to the injection site, in the contralateral Gi and paragigantocellular reticular nucleus. Some scattered varicosities were located in the ipsilateral SVN and MVN and extending rostrally into the PB. A more prominent projection was directed to the contralateral NRTP and BPN.

In the mesodiencephalon, the ventral part of the parvicellular part of the red nucleus was densely labeled. In addition, many terminals were noted in a region covering the rostral parts of the MA3, and extending into the prerubral field and adjacent area surrounding the fr and incorporating FF. Terminal arborizations were furthermore noted in a band aligning the ventrolateral margin of the APT. Additional labeling was noted in the posterior pretectal nucleus. A major projection was observed in the dorsal part of the ZI. Within the thalamus the most prominent labeling was observed in the medial parts of the VL, but, in addition, also within the PF, VM and Po.

Case R178

In this case, a PhaL injection was also centered on the ventral part of the LCN, however at distinctively more caudal levels compared to case T98 (Fig. 1). In fact, the injection appeared to be completely confined to the parvicellular part of the nucleus. In the PO, the ventral part of the lateral bend of the PO was densely labeled in the contralateral IO (Fig. 14, level 4). The ipsilateral IO also displayed a few corresponding labeled terminals. As can be discerned from Fig. 14 and the projection profile displayed in Fig. 8, the medulla oblongata showed no further labeling. The pons contained several structures with labeling contralateral to the injection site. Here, most distinct labeling was found in the caudal and dorsal boundaries of the NRTP, several patches in the lateral and medial parts of the BPN as well as a more scattered projection to the PnO and pedunculopontine tegmental nucleus.

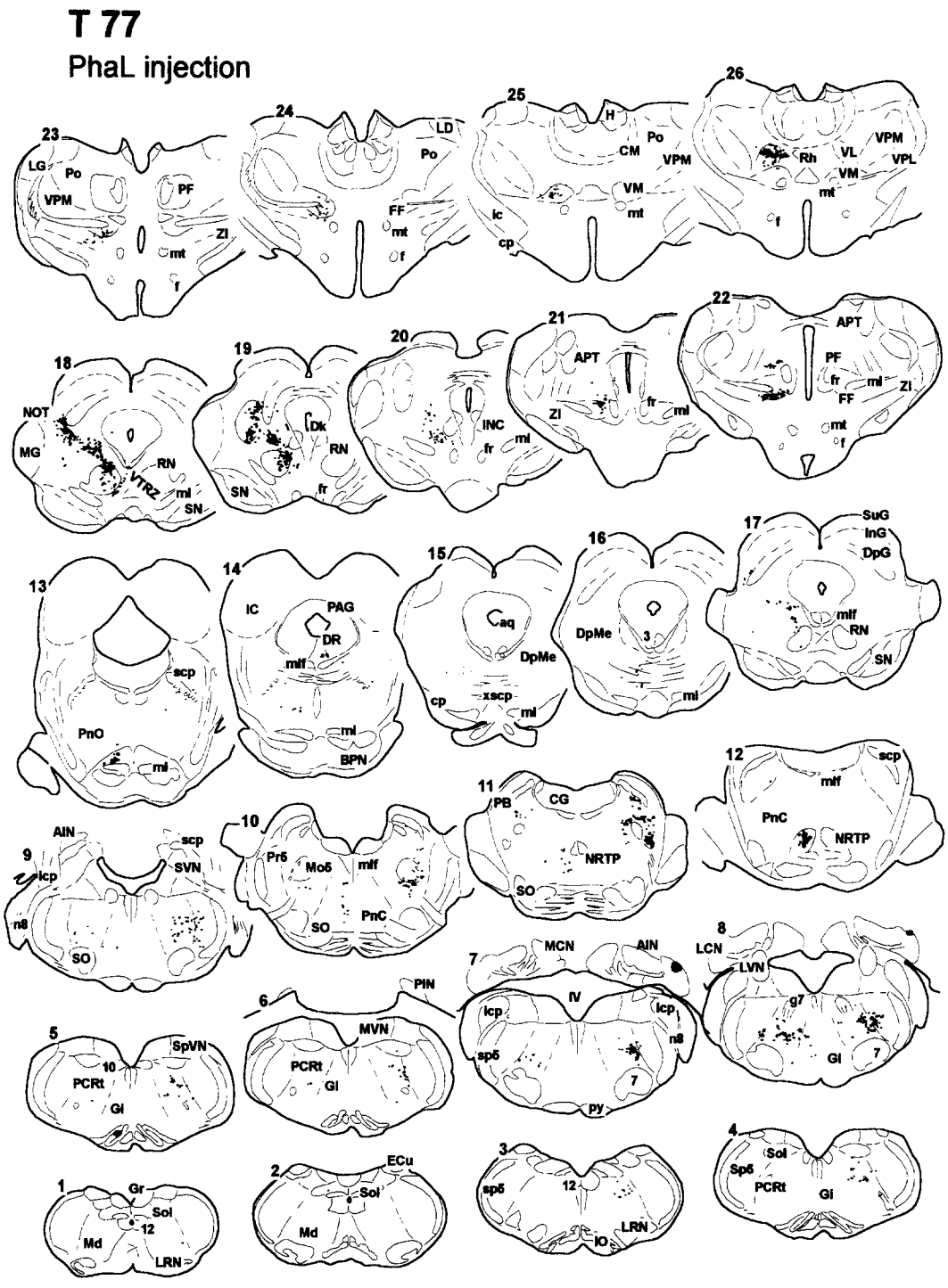

Fig. 12. Serial plots showing the distribution of labeled varicosities in case T77 with a PhaL injection centered on the dorsal tip of the rostral LCN. Further as Fig. 2.

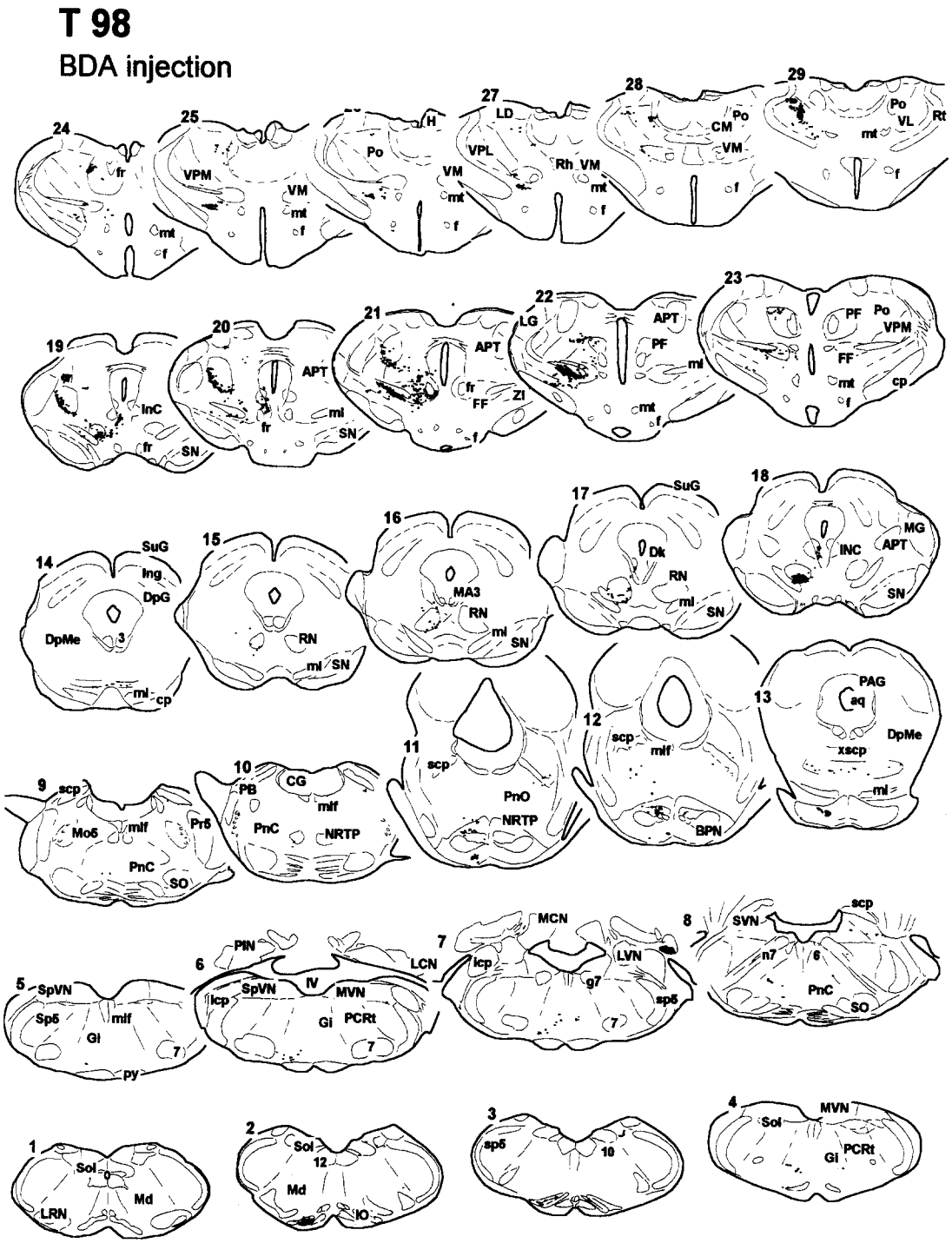

Fig. 13. Serial plots showing the distribution of labeled varicosities in case T98 with a BDA injection centered on the ventral half of the rostral LCN. Further as Fig. 2.

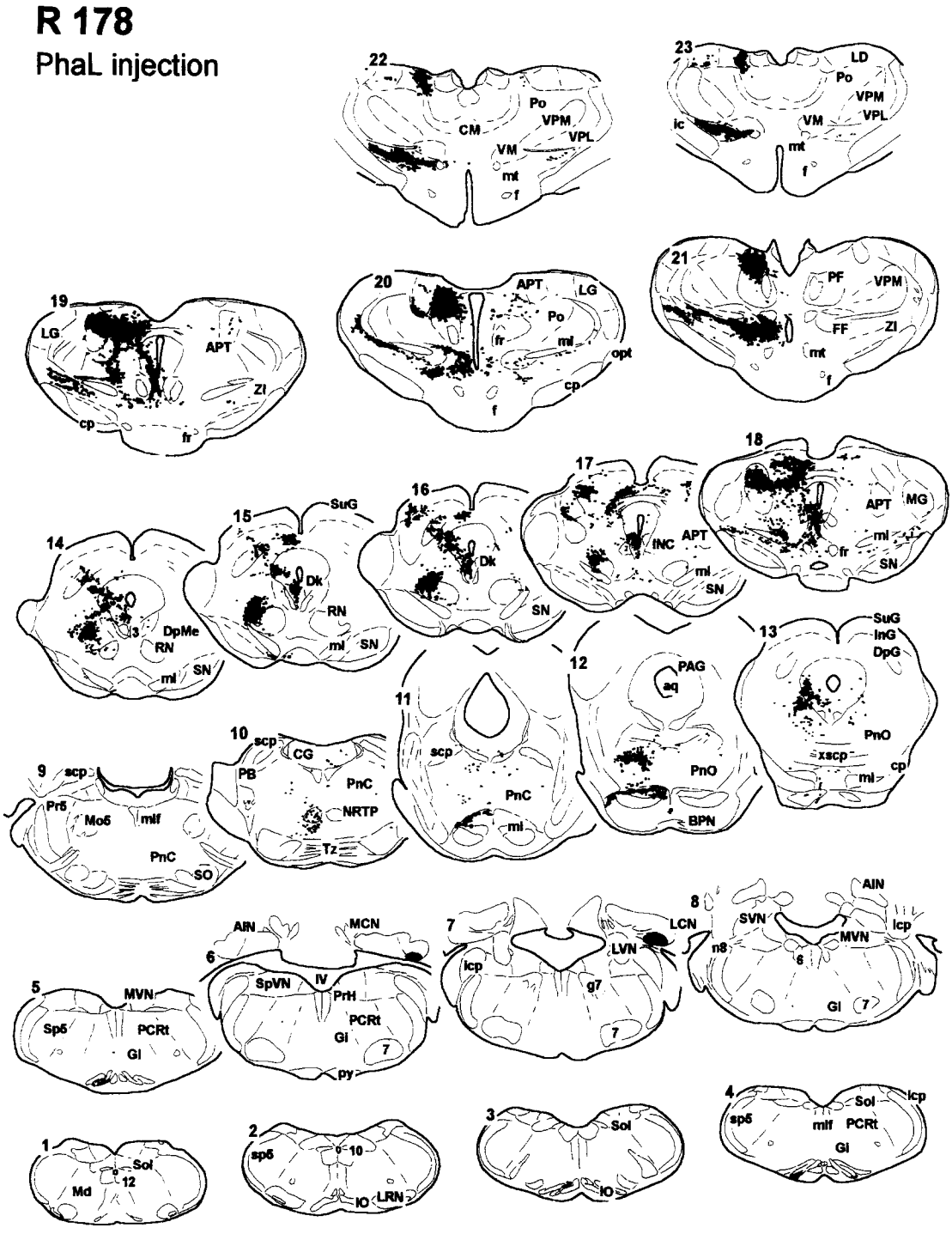

Fig. 14. Serial plots showing the distribution of labeled varicosities in case T178 with a PhaL injection centered on the ventral LCN. Further as Fig. 2.

Most terminals were directed to the mesodiencephalic region. In contrast with former cases, virtually all projections also displayed a small ipsilateral component. Particularly abundant projections were noted to reach all layers of the SC, the DpMe, the dorsal part of the APT, the nucleus of the posterior commissure, the MA3 and the PAG. Within the DpMe, a conspicuous aggregate of labeling was noted directly lateral to the magnocellular part of the RN, which, more rostrally converged with projections to the lateral part of the parvicellular part of the nucleus. For this reason, the area directly lateral to the magnocellular RN has been designated as the pararubral area (Ruigrok and Cella, 1995). Labeling to the parvicellular RN extended into the prerubral region and FF, where a prominent projection was noted (Fig. 14, levels 19–21). Dense terminal fields were also observed in the dorsal part of the ZI, with some patches extending into its ventral part. At the lateral margin of the ZI, labeled fibers bearing varicosities entered the confines of the ventral lateral geniculate nucleus. The ZI projections were especially abundant at the more rostral levels of this area where, medially, the terminal fields included the VM (Fig. 14, level 23). A very dense and salient patch of labeling was noted within the dorsal part of the PF. This terminal field extended into the medial parts of the LD group (levels 22,23). More laterally within this group some additional labeling was noted. Unfortunately, more rostral thalamic levels were not available for analysis. Case R178 also displayed a definite projection to dorsal and lateral hypothalamic regions. A few labeled varicosities were observed in the mammillary nuclei (Fig. 14, level 15).

Case T94

The PhaL injection of case T94 had been made dorsally in the caudal LCN bordering, but not involving, the DLH (Fig. 1). In the IO, the corresponding labeling remained confined to the ventral lamellae of the rostral PO without involvement of the DM group. Plots and the projection profile of this case are shown in Figs. 15 and 8, respectively.

At the medullary levels, this case was characterized by a strong projection to the contralateral Gi and paragigantocellular nucleus, extending ventrally into the region immediately dorsal to the inferior olive (into the ventral gigantocellular nucleus and nucleus gigantocellularis pars alpha of Jones, 1995), and medially to include the raphe nuclei. Some labeling was present in the ipsilateral PCRt and adjacent spinal trigeminal nucleus especially within its ventral margin. Projection patterns to the PnO, pedunculopontine tegmental nucleus, NRTP and BPN were very similar to those observed in case R178, however, projections were also noted in the PnC which appeared as a rostral continuation of the medullar Gi labeling. Patches with labeled varicosities were also seen laterally within the central gray of the pons. Also, some labeling was found in the ipsilateral A5 region (Fig. 15, level 11).

As in the former case, a large contingent of labeled varicosities were observed at the mesodiencephalic transition area. Major projections were noted to the MA3, PAG, pararubral area, DpMe, and APT. Also, the prerubral region and area surrounding the fr were studded with labeled varicosities, extending into the FF, ZI, and nucleus of the posterior commissure. As such the terminal arborizations within these areas appeared to be of a more or less continuous nature. In the thalamus, labeling was found in the PF (both dorsally and medially), within the VM, LD, and, most prominently, within the caudomedial regions of the VL. Finally, as in case R178, the lateral and dorsal hypothalamic area received a projection.

Discussion

The results presented here clearly show that small injections placed into selected parts of the CN invariably result in terminal projection patterns that are distributed over wide areas of the brain stem. It is likely that these output patterns relate to single cerebellar modules or submodules as based on intrinsic and olivocerebellar connections (Buisseret-Delmas and Angaut, 1993; Voogd et al., 1996). Moreover, the material shows that the projections to the IO are usually restricted to a single patch in one of its subdivisions indicating that in these cases the injection relates to a homogeneous olivocerebellar projection zone

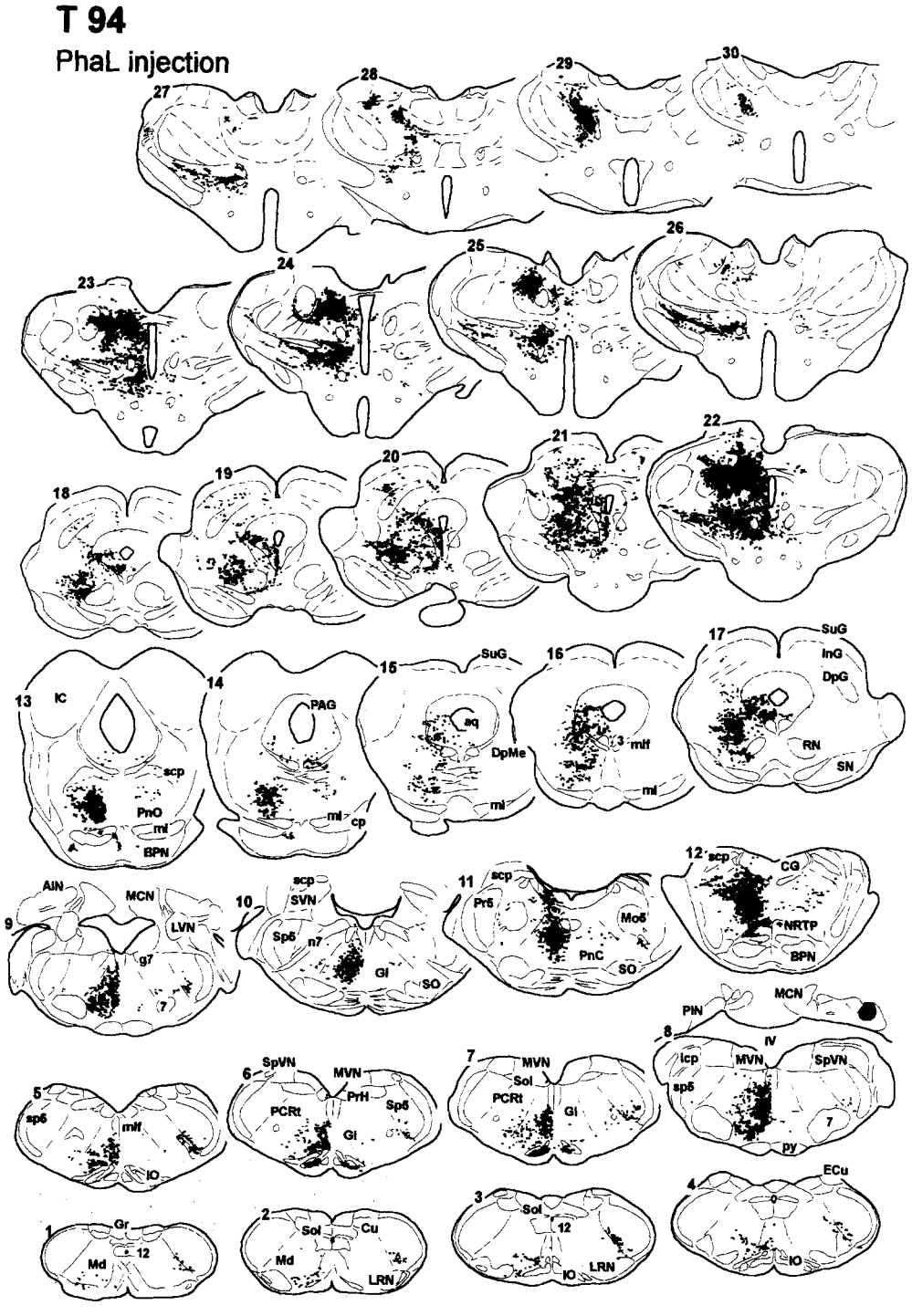

Fig. 15. Serial plots showing the distribution of labeled varicosities in case T94 with a PhaL injection centered on the caudal LCN. Further as Fig. 2.

(Ruigrok, 1997; Voogd, 1995). Hence, we conclude that the modular output is distributed to and processed in parallel in many brain stem areas.

Despite the great variety of brain stem structures that may be affected by the cerebellum, it would appear that most of them may be characterized as belonging to any of five basic groups. (1) The IO obviously functions as the source of cerebellar climbing fibers, with collaterals to all cerebellar target nuclei. The projections to different zones and their target nuclei do not seem to overlap and follow the patterns established previously (Ruigrok and Voogd, 1990; Ruigrok, 1997). (2) More diverse areas, such as the NRTP, BPN, LRN, etc. supply mossy fiber inputs. (3) In addition, as discussed above, several brain stem regions that receive a conspicuous cerebellar input, such as the medial mesodiencephalic region, pretectum, and DpMe, may serve as a source of IO input (Bull and Berkley, 1991; De Zeeuw and Ruigrok, 1994). (4) Several areas may be classified as 'effector' areas, e.g. such as the RN and supraoculomotor nuclei. Some effector regions, such as the vestibular nuclei, the SC and the reticular formation and the trigeminal nuclei, also serve as sources of mossy fiber input and as pre-olivary relay nuclei. (5) Finally, the thalamic projections of the CN should be considered. Some of them can be classified as belonging to cortical effector systems, others are part of complicated loops, involving the basal ganglia and/or precerebellar or effector regions in the brain stem. Since in the present study varicosities were plotted and counted, we noted that, in the rat, only a relatively low percentage ($<10\%$) of terminals were observed in the VL of the thalamus, which, nevertheless, is known as one of the classic termination areas of the CN. In fact, in many cases, most diencephalic terminals were observed in the ZI and/or the parafascicular thalamic nucleus.

From our results, it appears that it is difficult to clearly characterize the output of each cerebellar target nucleus unequivocally. Injections placed at various places in the same nucleus may show large differences in their terminal fields. For example, compare terminal fields and termination profiles of two MCN injections (R100 and T195) and the two PIN injections (T79 and T108). On the other hand, injections in different nuclei (e.g. the LCN in case T94 and the MCN in case R100) may show a basically similar distribution of terminal fields. Nevertheless, especially since the cerebellar modules and/or micromodules have been implicated to act as functional units it will be obvious that, in order to fully understand cerebellar functioning, the distributed nature of its modular output will have to be taken into account.

Cerebellar modules in the cat classically comprise the A, B, C1-C2-C3, D1 and D2 Purkinje cell zones (Voogd, 1964), which are connected to the MCN, lateral vestibular nucleus, AIN, PIN and dorsomedial and ventrolateral LCN, respectively. In the rat, additional zones were distinguished by Buisseret-Delmas and collaborators (Buisseret-Delmas, 1988a, b; Buisseret-Delmas and Angaut, 1989, 1993; Buisseret-Delmas et al., 1993) as will be detailed below. Here we will summarize and shortly review our main results from a modular point of view.

The A-module

The MCN serves as the target nucleus of the medial A zone of the vermis. The dorsolateral protuberance (DLP) of the rat MCN, however, is the target nucleus of a separate zone particular for rodents, the lateral extension of the A zone which is located in the medial hemisphere (Akaike, 1992; Buisseret-Delmas, 1988a). The caudal and rostral MCN and the DLP receive collaterals from different subnuclei of the caudal MAO. Rostral and caudal MCN receive collaterals from lateral subnucleus a, which relays somatosensory information from the cord and the dorsal column nuclei. The caudal MCN, in addition, receives collaterals from the subnucleus β, a vestibular relay nucleus and from subnucleus c (Akaike, 1992). The DLP receives collaterals from a different population of cells in subnucleus *c* of the caudal MAO, which project to the lateral extension of the A zone, but which shares SC afferents with the cells projecting to the vermal visual area located in lobule VII (Akaike, 1992).

The MCN is characterized by bilateral, but mainly crossed projections to the medial medullary and pontine reticular formation. In the case of the rostral MCN these are combined with strong,

bilateral projections to the vestibular nuclei. The DLP mostly lacks these vestibular projections. Its strong projections to the reticular formation involve the lateral PCRt and extend rostrally into pons and mesencephalon, where they include the DpMe, the INC, the PAG and the deep layers of the SC. Vestibular projections of the caudal MCN, which receives Purkinje cell axons from the vermal visual area (lobule VII) and lobules IX and X, are mostly restricted to the SVN. Its projections to brain stem includes several visual effector areas such as the nucleus prepositus hypoglossi, the pontine paramedian reticular formation, the supraoculomotor region, the SC, the INC, the MA3 and the rostral interstitial nucleus of the medial longitudinal fascicle, here considered part of the area parafascicularis prerubralis. The caudal MCN and the DLP provide the major thalamic projections of the MCN, with the PF and VM as their main targets. Terminations in precerebellar nuclei providing mossy fibers, such as the NRTP and the LRN, are rather sparse. Some overlap occurs in the projections to the reticular formation of the rostral MCN with the DLP and the caudal MCN. All subdivisions of the MCN share a projection to the parasolitary nucleus, which is a preolivary nucleus projecting to the subnucleus β and the dorsomedial cell column (Barmack et al., 1998). Potential overlap in the projections of the MCN with other CN is present in the medullary reticular formation (for rostral MCN with LCN), in the pontine reticular formation (for DLP and caudal MCN with caudal LCN) and in the DpMe (for DLP and caudal MCN with all CN), and in several of the visual effector areas targeted by the caudal MCN (with lateral PIN and ventral and caudal LCN).

The X-module

The interstitial cell groups (ICG) receive Purkinje cell axons from the X zone, located between the A and B zones of the anterior vermis (Yatim et al., 1995a, b). Its bulbar connections were recently discussed by Buisseret-Delmas and collaborators (Buisseret-Delmas et al., 1998); their conclusion that this nucleus receives climbing fiber collaterals from the DAO, in addition to the MAO, could not be substantiated in our experiments. Its projections to the reticular formation, the vestibular nuclei, the area prerubralis parafascicularis, prerubral field and ventrolateral thalamic nucleus may all overlap with those from other CN. A sparse projection to the caudal RN could be confirmed, and a small focus of termination was observed in the NRTP in our case T82. One of the main, and relatively exclusive, connections of the ICG with the contralateral spinal cord (Bentivoglio and Kuypers, 1982; Horn et al., 1995) was not studied in our material or that of Buisseret-Delmas et al. (1998). According to Bentivoglio and Kuypers (1982) ICG neurons may collateralize to both the spinal cord and the thalamus.

The B-module

The lateral vestibular nucleus of Deiters (LVN), which serves as the target nucleus of the lateral B zone of the anterior vermis, has not been studied in this paper. Its Purkinje cells receive their climbing fiber input from the dorsal fold of the DAO which also provides a collateral projection to the LVN. The LVN gives rise to the lateral vestibulospinal tract (Rubertone et al., 1995).

The C2-module

The PIN is target nucleus of the C2 zone (Voogd and Bigaré, 1980). In the rat, however, the projection of the C1 and C3 zones includes the medial AIN and PIN, and the lateral AIN, respectively. C2 projects to intermediate AIN and lateral PIN (Buisseret-Delmas, 1988b). Climbing fiber afferents result from DAO for C1 and C3 and from rostral MAO for C2. In our material, however, injections placed in both medial (T79) and lateral PIN (T108) project to MAO and not to DAO, whereas injections in medial AIN (R89) failed to result in terminal labeling within the MAO, suggesting that the olivo-cortico-nucleo-olivary circuits may not be closed. The PIN scarcely connects with the medulla and the pons, apart from its reciprocal connections with the rostral MAO. The rostral MAO is one of the main targets of the preolivary neurons in the area parafascicularis prerubralis. The RN receives a projection from the medial PIN, located along the medial border of the

nucleus. It is not clear whether these terminals overlap with projections from other CN, such as the AIN or the LCN; a projection to the NRTP seems to be lacking. Several of its projections to mes- and diencephalon, especially those from lateral PIN, overlap with those from the ventral and caudal LCN, and less so, with the caudal MCN (SC, the PAG, the nucleus of the posterior commissure, the area parafascicularis prerubralis and the VL). Its projection to the ZI is shared by most CN, with the exception of the MCN.

The C1- and C3-modules

The AIN is the target nucleus of the C1 and C3 zones. It receives collaterals from the DAO, which is the main somatosensory relay nucleus of the IO. The head is represented in the lateral part of the AIN and the hindlimbs in its medial part (Gellman et al., 1983). Strict somatotopical projections are noted to the magnocellular part of the RN and to the DAO (Daniel et al., 1987); the medial AIN connects to the ventrolateral RN and rostromedial DAO. Other main projections are directed to the NRTP, the APT, the ZI and the thalamus. In the VL nucleus of the thalamus its terminals are typically located laterally, segregated from the other CN; they presumably relay information of a somatosensory nature to the motor cortex. The APT, which is the recipient of a major part of the AIN efferents, gives rise to a projection to the ipsilateral IO, which, in the cat, terminates in the rostral DAO (Bull et al., 1990). Ipsilaterally descending projections to the PCRt and adjacent deep layers of the spinal trigeminal nucleus specifically arise from the lateral AIN (R98).

The D0-module

The dorsolateral hump (DLH) is the target nucleus of the D0 zone (Buisseret-Delmas and Angaut, 1993). There is no clear equivalent of this zone in either cats or monkeys. The DLH is reciprocally connected with the dorsomedial group of the IO (Ruigrok and Voogd, 1990; Ruigrok, 1997). Afferents from the trigeminal nuclei and adjacent reticular formation terminate in this olivary subnucleus (see Ruigrok and Cella, 1995 for a review). The rodent DLH is characterized by a unique ipsilateral projection to the PCRt, the pontine reticular formation and the trigeminal nuclei (Woodson and Angaut, 1984). Neurons with similar projections are present in the adjacent lateral AIN and dorsomedial LCN, some of which also include a contralateral component (Bentivoglio and Kuypers, 1982). Crossed projections to RN, NRTP, DpMe and APT are shared with the adjacent CN; the terminations in the thalamus are mostly restricted to the intralaminar nuclei.

The D1- and D2-modules

The LCN is the target nucleus of the D1 and the D2 zones. In the rat, Purkinje cells of these zones terminate in the rostral and dorsal, and the ventral and caudal parts of the LCN, respectively (Buisseret and Angaut, 1993). The rostral and dorsal parts of the LCN receive collaterals from the dorsal leaf of the PO; the ventral and caudal part of the nucleus from the ventral leaf. The connections of the D1 and D2 zones in rodents and in carnivores appear to be reversed. In the cat, the ventral leaf of the principal olive provides climbing fibers to the medial D1 zone and collaterals to its target nucleus, the caudolateral LCN and the dorsal leaf innervates the lateral D2 zone and its target nucleus, the rostral, dorsomedial LCN (Voogd and Bigaré, 1980).

The rostral and dorsomedial and the caudal and ventral LCN display clear differences in their projection. Bilateral projections of the rostral LCN to the reticular formation and the trigeminal nuclei resemble the adjacent DLH. Strong projections to the ventromedial medullary reticular formation, which overlap with MCN projections, are characteristic of the caudal LCN. All subdivisions of the LCN give rise to projections to the DpMe, the parvicellular part of the RN, the APT, the prerubral field, the parafascicular prerubral area, the ZI and the VM and VL of the thalamus. The terminal field of the rostral LCN in the RN includes its magnocellular part, whereas the caudal LCN provides a strong projection to the pararubral area. The terminal field in the APT extends into lateral and dorsal parts of the nucleus. Projections to visual effector areas mainly arise from the caudal LCN;

these terminations in SC, the MA3, the PAG, and the area parafascicularis prerubralis may partially overlap with the caudal MCN and the lateral PIN. In the paralaminar, medial VL nucleus of the thalamus, the caudal LCN projection overlaps with the PIN (Aumann et al., 1994; Aumann et al., 1996).

Summary and conclusions

The organization of the cerebellum is characterized by a number of parallel and parasagittally ordered olivocorticonuclear modules; as such, the cerebellar nuclei basically function as output system of these modules. The present study provides a comprehensive and detailed description of the organization of the connections from the cerebellar nuclei to the brain stem in the rat. Thirteen small injections with the anterograde tracer *Phaseolus vulgaris* leucoagglutinin or biotinylated dextran amine which were centered on various aspects of the cerebellar nuclear complex are described and are illustrated with serial plots detailing the distribution of labeled varicosities throughout the brain stem. In every case at least 1,000 and up to 36,000 varicosities were plotted.

All injections resulted in some or heavy labeling concentrated within specific regions of the contralateral inferior olivary complex and, usually, in some labeling of the contralateral ventrolateral thalamus. However, apart from these two areas it is shown that the cerebellar projections are generally very widespread and may be found throughout the entire brain stem. Below, only a survey of main projection areas will be given. Terminal arborizations originating from the rostral part of the medial cerebellar nucleus are mostly found in the caudal half of the brain stem with emphasis on the vestibular nuclear complex, whereas its caudal part rather connects to midbrain areas. Terminals that originate from the dorsolateral protuberance of the medial cerebellar nucleus are distributed more evenly throughout the brain stem and are mostly confined to reticular areas. The interstitial cell groups, interspersed between the medial and both interposed cerebellar nuclei, provide major projections to the ipsilateral vestibular nuclear complex and contralateral mesodiencephalic regions. However, reticular areas are also targeted over a large rostrocaudal range. The medial part of the posterior interposed nucleus sends most projections to the caudomedial red nucleus, prerubral regions and parvicellular reticular formation, all contralateral to the injection site. Projections that originate from more laterally placed injections are directed, apart from the inferior olivary complex, to the rostral half of the contralateral brain stem, where most labeled varicosities are found in the superior colliculus and zona incerta. The anterior interposed nucleus specifically targets the inferior olive, the red nucleus, the pontine reticulotegmental nucleus, the prectectum and the ventrolateral thalamic nucleus. More laterally placed injections also project to the ipsilateral parvicellular reticular formation and deep layers of the spinal trigeminal complex. The latter areas are more specifically targeted by the dorsolateral hump. In addition, its projections are found in the red nucleus and pretectum but do not seem to reach the ventrolateral thalamus. Projections from the lateral cerebellar nucleus are all characterized by a widespread distribution of terminals. Especially, the caudal aspect of the nucleus sends, apart from projections to the deep mesencephalic nucleus, red nucleus, periaquaductal gray, pretectum, prerubral area, and several thalamic regions, prominent projections to the caudal brain stem which terminate in the inferior olive and gigantocellular reticular formation. Projections from the ventral, parvicellular part of the nucleus are mostly, but not exclusively, directed to the rostral half of the brain stem and mainly terminate in the pararubral area, accessory oculomotor nuclei, pretectal areas, zona incerta, and in the parafascicular and ventrolateral thalamic nuclei.

We conclude that the impact of the cerebellar nuclei on the brain stem is widespread; projections from different regions of the same cerebellar nucleus may show important differences in distribution of labeled terminals. On the other hand, injections placed in different cerebellar nuclei may result in a similar distribution of at least part of their terminal fields. Hence, complex divergence and convergence between and within the projections of individual cerebellar nuclei appear to be an essential characteristic of the cerebellar nucleobulbar organization.

Acknowledgements

The authors express their gratitude to Mr. E. Dalm and Mrs. E. Sabel-Goedknegt for their excellent technical assistence. T.M. Teune was supported by NWO grant 903–47–005.

List of abbreviations

3	oculomotor nucleus
6	abducens nucleus
7	facial nucleus
10	vagal motor nucleus
12	hypoglossal nucleus
A	anterior thalamic nucleus
A5	A5 noradrenaline cells
AIN	anterior interposed nucleus
Amb	ambiguus nucleus
APT	anterior pretectal nucleus
aq	aquaduct
BDA	biotinylated dextran amine
BPN	basilar pontine nuclei
Cg	central gray
CM	centromedial nucleus
CN	cerebellar nuclei
cp	cerebral peduncle
Cu	cuneate nucleus
DAO	dorsal accessory olive
Dk	nucleus of Darkschewitsch
DLH	dorsolateral hump
DLP	dorsolateral protuberance
DM	dorsomedial group
DpG	deep gray layer SC
DpMe	deep mesencephalic nuclei
Ecu	external cuneate nucleus
f	fornix
FF	field of Forel
fr	fasciculus retroflexus
g7	genu of facial nerve
Gi	gigantocellular reticular nucleus
Gr	gracile nucleus
H	habenula
ic	internal capsule
IC	inferior colliculus
ICG	interstitial cell groups
icp	inferior cerebellar peduncle
III	third ventricle
INC	interstitial nucleus of Cajal
InG	intermediate gray layer SC
IO	inferior olive
IV	fourth ventricle
LCN	lateral cerebellar nucleus
LD	laterodorsal thalamic nucleus
LG	lateral geniculate nucleus
LRN	lateral reticular nucleus
LVN	lateral vestibular nucleus
MA3	medial accessory oculomotor nucleus
MAO	medial accessory olive
MCN	medial cerebellar nucleus
mcp	medial cerebellar peduncle
Md	medullary reticular nucleus
Me5	mesencephalic trigeminal nucleus
MG	medial geniculate nucleus
ml	medial lemiscus
mlf	medial longitudinal fascicle
Mo5	motor trigeminal nucleus
mp	mammillary peduncle
mt	mammillothalamic tract
n7	facial nerve
n8	vestibulocochlear nerve
NOT	nucleus of the optic tract
NRTP	nucleus reticularis tegmenti pontis
opt	optic nerve
Pa	paraventricular hypothalamic nucleus
PAG	periaquaductal gray
PB	parabrachial nuclei
pc	posterior commissure
PCRt	parvicellular reticular formation
PF	parafascicular thalamic nucleus
PhaL	Phaseolus vulgaris-leucoagglutinin
PIN	posterior interposed nucleus
PnC	caudal pontine reticular formation
PnO	oral pontine reticular formation
Po	posterior thalamic nucleus
PO	principal olivary nucleus
Pr5	principal sensory trigeminal nucleus
PrH	prepositus hypoglossal nucleus
py	pyramidal tract
Rh	Rhomboid nucleus
RI	rostral interstitial nucleus
RN	red nucleus
Rt	reticular thalamic nucleus
SC	superior colliculus
scp	superior cerebellar peduncle
SN	substantia nigra

SO	superior olive
Sol	nucleus of solitary tract
Sp5	spinal trigeminal nucleus
sp5	spinal trigeminal tract
SpVN	spinal vestibular nucleus
STh	subthalamic nucleus
SuG	superficial gray layer SC
SVN	superior vestibular nucleus
Tz	trapezoid body
VL	ventrolateral thalamic nucleus
VM	ventromedial thalamic nucleus
VPL	ventral posterolateral thalamic nucleus
VPM	ventral posteromedial thalamic nucleus
VTRZ	visual tegmental relay zone
xopt	optic chiasm
xpy	decussation of py
xscp	decussation of scp
ZI	zona incerta

References

Akaike, T. (1992) The tectorecipient zone in the inferior olivary nucleus in the rat. *J. Comp. Neurol.*, 320: 398–414.

Angaut, P., Cicirata, F. and Pantò, M.-R. (1985a) An autoradiographic study of the cerebellopontine projections from the interposed and lateral cerebellar nuclei in the rat. *J. Hirnforsch.*, 26: 463–470.

Angaut, P., Cicirata, F. and Serapide, F. (1985b) Topographic organization of the cerebellothalamic projections in the rat: an autoradiographic study. *Neuroscience*, 15: 389–401.

Angaut, P., Cicirata, F. and Serapide, M.F. (1987) The dentatorubral projection: an autoradiographic study in rats. *Brain Behav. Evol.*, 30: 272–281.

Asanuma, C., Thach, W.T. and Jones, E.G. (1983) Brainstem and spinal projections of the deep cerebellar nuclei in the monkey, with observations on the brainstem projections of the dorsal column nuclei. *Brain Res. Rev.*, 5: 299–322.

Aumann, T.D., Rawson, J.A., Finkelstein, D.I. and Horne, M.K. (1994) Projections from the lateral and interposed cerebellar nuclei to the thalamus of the rat: a light and electron microscopic study using single and double anterograde labelling. *J. Comp. Neurol.*, 349: 165–181.

Aumann, T.D., Rawson, J.A., Pichitpornchai, C. and Horne, M.K. (1996) Projections from the cerebellar interposed and dorsal column nuclei to the thalamus in the rat: a double anterograde labelling study. *J. Comp. Neurol.*, 368: 608–619.

Barmack, N.H., Fredette, B.J. and Mugnaini, E. (1998) Parasolitary nucleus: a source of GABAergic vestibular information to the inferior olive of rat and rabbit. *J. Comp. Neurol.*, 392: 352–72.

Bentivoglio, M. and Kuypers, H.G.J.M. (1982) Divergent axon colaterals from rat cerebellar nuclei to diencephalon, mesencephalon, medulla oblongata and cervical cord. *Exp. Brain Res.*, 46: 339–356.

Bloedel, J.R. (1992) Functional heterogeneity with structural homogeneity: how does the cerebellum operate? *Behav. Brain Sci.*, 15: 666–678.

Bradley, D.J., Paton, J.F.R. and Spyer, K.M. (1987) Cardiovascular and respiratory responses evoked from the posterior cerebellar cortex and fastigial nucleus in the cat. *J. Physiol. (Lond.)*, 393: 107–121.

Buisseret-Delmas, C. (1988a) Sagittal organization of the olivocerebellonuclear pathway in the rat. I. Connections with the nucleus fastigii and the nucleus vestibularis lateralis. *Neurosci. Res.*, 5: 475–493.

Buisseret-Delmas, C. (1988b) Sagittal organization of the olivocerebellonuclear pathway in the rat. II. Connections with the nucleus interpositus. *Neurosci. Res.*, 5: 494–512.

Buisseret-Delmas, C. and Angaut, P. (1989) Sagittal organization of the olivocerebellonuclear pathway in the rat. III. Connections with the nucleus dentatus. *Neurosci. Res.*, 7: 131–143.

Buisseret-Delmas, C. and Angaut, P. (1993) The cerebellar olivo-cortico-nuclear connections in the rat. *Progr. Neurobiol.*, 40: 63–87.

Buisseret-Delmas, C., Angaut, P., Compoint, C., Diagne, M. and Buisseret, P. (1998) Brainstem efferents from the interface between the nucleus medialis and the nucleus interpositus in the rat. *J. Comp. Neurol.*, 402: 264–275.

Buisseret-Delmas, C., Yatim, N., Buisseret, P. and Angaut, P. (1993) The X zone and CX subzone of the cerebellum in the rat. *Neurosci. Res.*, 16: 195–207.

Bull, M.S. and Berkley, K.J. (1991) Cerebellar projections to the somatic pretectum in the cat. *Somatosens. Motor Res.*, 8: 117–126.

Bull, M.S., Mitchell, S.K. and Berkley, K.J. (1990) Convergent inputs to the inferior olive from the dorsal column nuclei and pretectum in the cat. *Brain Res.*, 525: 1–10.

Carlton, S.M., Leichnetz, G.R. and Mayer, D.J. (1982) Projections from the nucleus parafascicularis prerubralis to medullary raphe nuclei and inferior olive in the rat: a horseradish peroxidase and autoradiography study. *Neurosci. Lett.*, 30: 191–197.

Chan-Palay, V. (1977) *Cerebellar Dentate Nucleus: Organization, Cytology and Transmitters*. Springer-Verlag, Berlin.

Cicirata, F., Panto, M.R. and Angaut, P. (1982) An autoradiographic study of the cerebellopontine projections in the rat. I. Projections from the medial cerebellar nucleus. *Brain Res.*, 253: 303–308.

Daniel, H., Billard, J.M., Angaut, P. and Batini, C. (1987) The interposito-rubrospinal system: anatomical tracing of a motor control pathway in the rat. *Neurosci. Res.*, 5: 87–112.

De Zeeuw, C.I. and Ruigrok, T.J.H. (1994) Olivary projecting neurons in the nucleus of Darkschewitsch in the cat receive

excitatory monosynaptic input from the cerebellar nuclei. *Brain Res.*, 653: 345–350.

Ekerot, C.-F., Jorntell, H. and Garwicz, M. (1995) Functional relation between corticonuclear input and movements evoked on microstimulation in cerebellar nucleus interpositus anterior in the cat. *Exp. Brain Res.*, 106: 365–376.

Faull, R.L.M. (1978) The cerebellofugal projections in the brachium conjunctivum of the rat. II. The ipsilateral and contralateral descending pathways. *J. Comp. Neurol.*, 178: 519–536.

Faull, R.L.M. and Carman, J.B. (1978) The cerebellofugal projections in the brachium conjunctivum of the rat. I. The contralateral ascending pathway. *J. Comp. Neurol.*, 178: 495–518.

Gellman, R., Houk, J.C. and Gibson, A.R. (1983) Somatosensory properties of the inferior olive of the cat. *J. Comp. Neurol.*, 215: 228–243.

Godschalk, M., Van der Burg, J., Van Duin, B. and De Zeeuw, C.I. (1994) Topography of saccadic eye movements evoked by microstimulation in rabbit cerebellar vermis. *J. Physiol.*, 480: 147–153.

Haines, D.E., May, P.J. and Dietrichs, E. (1990) Neuronal connections between the cerebellar nuclei and hypothalamus in *Macaca fascicularis*: cerebello-visceral circuits. *J. Comp. Neurol.*, 299: 106–122.

Haroian, A.J., Massopust, L.C. and Young, P.A. (1981) Cerebellothalamic projections in the rat: an autoradiographic and degeneration study. *J. Comp. Neurol.*, 197: 217–236.

Horn, K.M., Porter, C.M. and Gibson, A.R. (1995) Spinal connections of cat posterior interpositus. *Soc. Neurosci. Abstr.*, 21: 1190.

Ito, M. (1984) *The Cerebellum and Neural Control*, Raven Press, New York.

Jones, B.E. (1995) Reticular formation: cytoarchitecture, transmitters, and projections. In: G. Paxinos (Ed.), *The Rat Central Nervous System*, Academic Press, New York, pp. 155–171.

Korneliussen, H.K. (1968) On the morphology and subdivision of the cerebellar nuclei of the rat. *J. Hirnsforsch.*, 10: 109–122.

Leiner, H.C., Leiner, H.C. and Dow, R.S. (1986) Does the cerebellum contribute to mental skills? *Behav. Neurosci.*, 100: 443–454.

Nisimaru, N., Okahara, K. and Nagao, S. (1991) Olivocerebellar projection to the cardiovascular zone of rabbit cerebellum. *Neurosci. Res.*, 12: 240–250.

Oscarsson, O. (1969) The sagittal organization of the cerebellar anterior lobe as revealed by the projection patterns of the climbing fiber system. In: R. Llinas (Ed.), *Neurobiology of Cerebellar Evolution and Development*, AMA-ERF, Chicago, pp. 525–537.

Oscarsson, O. (1979) Functional units of the cerebellum – sagittal zones and microzones. *TINS*, 2: 143–145.

Paxinos, G. and Watson, C. (1986) *The Rat Brain in Stereotaxic Coordinates*, Academic Press, Sidney.

Rubertone, J.A., Mehler, W.R. and Voogd, J. (1995) The vestibular nuclear complex. In: G. Paxinos (Ed.), *The Rat Central Nervous System*, Academic Press, Sydney, pp. 773–796.

Ruigrok, T.J.H. (1997) Cerebellar nuclei: the olivary connection. In: C.I. De Zeeuw, P. Strata, J. Voogd (Ed.), *The Cerebellum: from Structure to Control*, Elsevier Science B.V., pp. 162–197.

Ruigrok, T.J.H. and Cella, F. (1995) Precerebellar nuclei and red nucleus. In: G. Paxinos (Ed.), *The Rat Central Nervous System*, Academic Press, Sydney, pp. 277–308.

Ruigrok, T.J.H. and Voogd, J. (1990) Cerebellar nucleo-olivary projections in rat. An anterograde tracing study with *Phaseolus vulgaris*-leucoagglutinin (PHA-L). *J. Comp. Neurol.*, 298: 315–333.

Schmahmann, J.D. (1996) From movement to thought: anatomic substrates of the cerebellar contribution to cognitive processing. *Hum. Brain Mapp*, 4: 174–198.

Teune, T.M., van der Burg, J., De Zeeuw, C.I., Voogd, J. and Ruigrok, T.J.H. (1998) Single Purkinje cell can innervate multiple classes of projection neurons in the cerebellar nuclei of the rat: a light microscopic and ultrastructural triple-tracer study in the rat. *J. Comp. Neurol.*, 392: 164–178.

Thach, W.T. (1996) On the specific role of the cerebellum in motor learning and cognition: clues from PET activation and lesion studies in man. *Behav. Brain Sci.*. 19: 411.

Tolbert, D.L., Bantli, H. and Bloedel, J.R. (1978) Organizational features of the cat and monkey cerebellar nucleocortical projection. *J. Comp. Neurol.*, 182: 39–56.

van der Steen, J., Simpson, J.I. and Tan, J. (1994) Functional and anatomic organization of three-dimensional eye movements in rabbit cerebellar flocculus. *J. Neurophysiol.*, 72: 31–46.

Voogd, J. (1964) *The Cerebellum of the Cat: Structure and Fiber Connections*, Van Gorcum, Assen.

Voogd, J. (1995) The cerebellum. In: G. Paxinos (Ed.), *The Rat Central Nervous System*, Academic Press, Sydney, pp. 309–350.

Voogd, J. and Bigaré, F. (1980) Topographical distribution of olivary and cortico nuclear fibers in the cerebellum: a review. In: J. Courville, C. de Montigny, Y. Lamarre (Eds), *The Inferior Olivary Nucleus: Anatomy and Physiology*, Raven Press, New York, pp. 207–234.

Voogd, J., Jaarsma, D. and Marani, E. (1996) The cerebellum: chemoarchitecture and anatomy. In: L.W. Swanson, A. Björklund, T. Hökfelt (Eds), *Handbook of Chemical Neuroanatomy*, Elsevier Sience B.V., pp. 1–369.

Waldrop, T.G. and Iwamoto, G.A. (1991) Cardiovascular responses to chemical stimulation of the inferior olive in the cat. *Brain Res. Bull.*, 26: 667–670.

Woodson, W. and Angaut, P. (1984) The distribution and origin of the ipsilateral descending limb of the brachium conjunctivum. An autoradiographic and horseradish peroxidase study in the rat. *Exp. Brain Res.*, 56: 167–182.

Wouterlood, F.G. and Groenewegen, H.J. (1985) Neuroanatomical tracing by use of Phaseolus vulgaris – leucoagglutinin

(Pha-L): electron microscopy of Pha-L filled neuronal somata, dendrites, axons and axon terminals. *Brain Res.*, 326: 188–181.

Wouterlood, F.G. and Jorritsma-Byham, B. (1993) The anterograde neuroanatomical tracer biotinylated dextran-amine: comparison with the tracer *Phaseolus vulgaris*-leucoagglutinin in preparations for electron microscopy. *J. Neurosci. Meth.*, 48: 75–87.

Yatim, N., Buisseret-Delmas, C., Buisseret, P., Compoint, C. and Angaut, P. (1995a) Nucleus medialis-nucleus interpositus interface: its olivary and cerebellocortical projections in the rat. *J. Comp. Neurol.*, 363: 1–14.

Yatim, N., Compoint, C., Buisseret, P., Angaut, P. and Buisseret-Delmas, C. (1995b) On the caudal extension of the X zone in the cerebellar cortex of the rat. *Neurosci. Res.*, 23: 223–227.